2020 Introduction to Fusion Energy and Plasma Physics Course

Plasma-Material Interaction: Boundary Plasmas

Professor David Donovan
ddonovan@utk.edu
Department of Nuclear Engineering
University of Tennessee-Knoxville
USA

THE UNIVERSITY OF TENNESSEE KNOXVILLE

My research journey started with a SULI internship at ORNL with people I still work with today

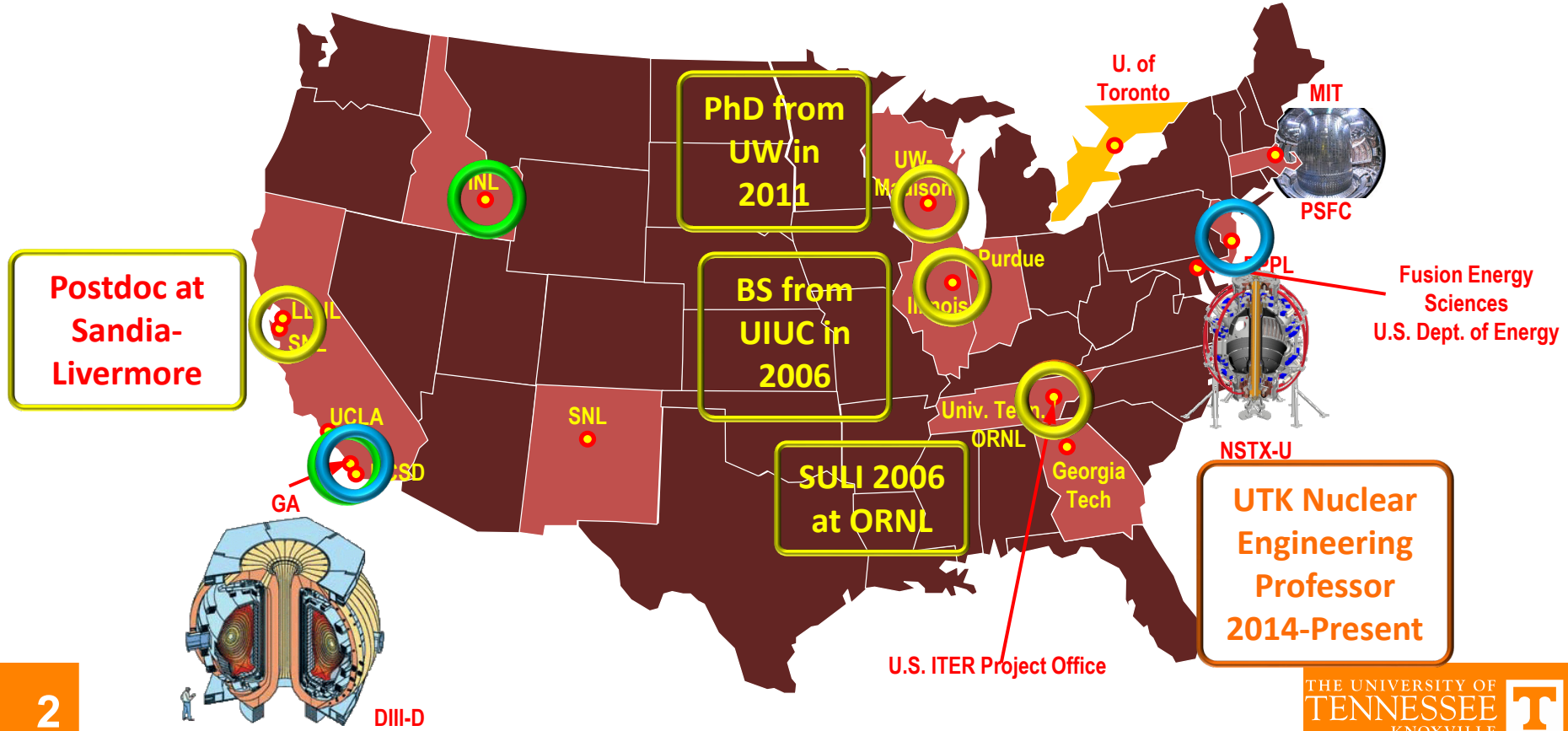

UTNE Fusion Technology program focuses on PMI challenges with experimental and computational research

University of Tennessee Nuclear Engineering (UTNE) Department

Fusion Faculty

Dr. David Donovan

Dr. Brian Wirth

Dr. Steven Zinkle

Themes

- Advanced computational modeling and experimental characterization of plasma surface interactions and structural materials response from burning fusion plasma conditions.
- Characterizing and understanding radiation damage to materials in fusion neutron environments.
- Developing diagnostics for plasma boundary and plasma material interactions, in addition to experimental plasma physics & material characterization

Accomplishments

- Experiments & modeling tungsten surface response to low-energy plasma exposure and evaluating hydrogen retention at sub-surface bubbles
- Developing laser-based plasma diagnostics, as well as diagnostics for plasma boundary in fusion reactors
- Development of laboratory-based plasma source assessing microstructure stability and radiation performance of novel structural materials for fusion

Activities

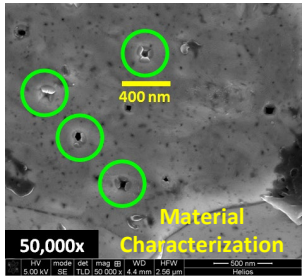

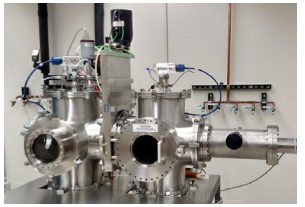

Plasma Exposure Stage

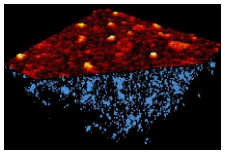

Advanced Computational Molecular Dynamics Modelling

Experimental boundary plasma and PMI research has grown rapidly through collaborations and campus development

Campus Development and Capabilities

- **UTNE Plasma Exposure Stage** developed for low flux (10^{18}-10^{19} ions/m^2 sec) He/H ion damage studies to PFC candidate materials.
  - Compact ECR plasma source and heated stage (≤1000° C).
  - He ion exposure to WO_3 films performed in collaboration with U. of Marseilles (Hijazi, et al., JNM 484, 91 (2017))
- Variety of **material characterization** techniques available within the Nuclear Engineering, Material Science, and Physics Departments at UTK.
  - Ion Beam Laboratory (RBS, NRA, ion implantation)
  - Scanning Tunneling Microscopy (STM)
  - Atomic Force Microscopy (AFM)
  - Optical Profilometry
  - Grazing Incidence X-Ray Diffraction (GIXRD)
  - Electron Backscatter Diffraction (EBSD)
- **UT Institute for Nuclear Security** (http://nuclear.utk.edu/)
  - Radiochemistry laboratories capable of wide variety of wet chemistry and rated for radioactive materials (including tritium).
  - Inductively Coupled Plasma Time-of-Flight Mass Spectroscopy (ICP-TOF-MS) system used for isotopic and elemental analysis for 2016 DIII-D Metal Tile Campaign.

UTNE Plasma Exposure Stage

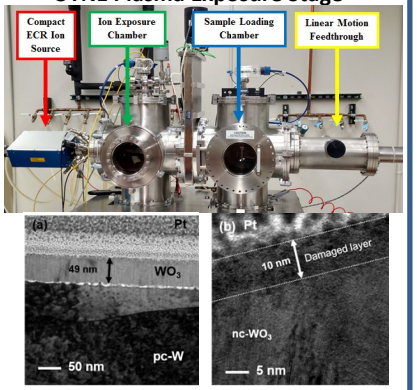

WO_3-He673K sample: (a) TEM image (b) high resolution TEM image showing the formation of a darker layer on the oxide surface.

Chemical dissolutions and ICP-MS analysis of DIII-D collector probes

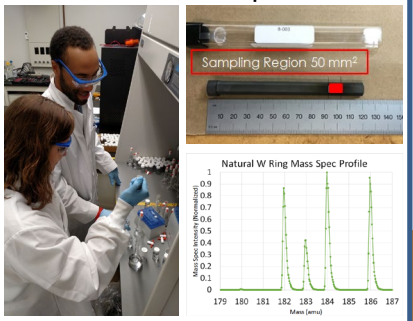

Experimental boundary plasma and PMI research has grown rapidly through collaborations and campus development

Research Collaborations

- Prototype Material Plasma Exposure Stage (**Proto-MPEX**) (ORNL) involved 2 UTK PhD Students working on: Plasma transport and plasma diagnostics (Langmuir probes, Thomson scattering), Heat flux diagnostics and power balance
- Lithium Tokamak Experiment (**LTX-Beta**) (PPPL) involved 1 UTK PhD student.
  - Surface chemistry (XPS, RBS, NRA) and boundary plasma studies
- **NSTX-U** (PPPL) involves 1 UTK PhD student developing machine learning tools for surface heat flux analysis.
- **DIII-D** (GA) involves 3 graduate students, 2 undergraduate students, 1 postdoc. (Support from DE-SC0016318)
  - Elemental/Isotopic analysis for impurity transport studies, development of collector probes.
  - Analysis of plasma conditions from Metal Tile Campaign and planning of future DIII-D experiments and diagnostic implementation.
  - Design and implementation of new heat flux diagnostics and ion energy distribution measurements.
- **WEST** Experiment (CEA) in Cadarache, France involves 2 UTK PhD students.
  - Impurity transport studies in a high-Z walled long pulse device.

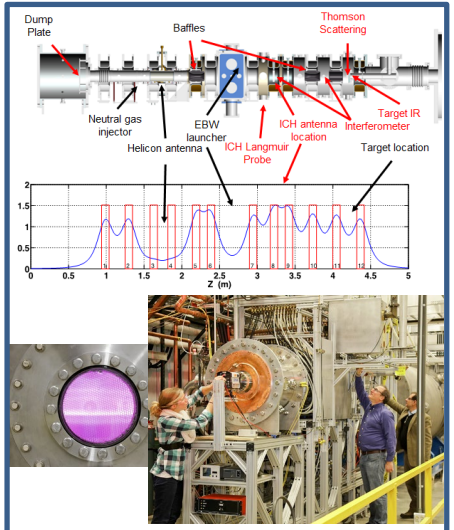

M. Showers (left) calibrating IR Camera on Proto-MPEX (ORNL)

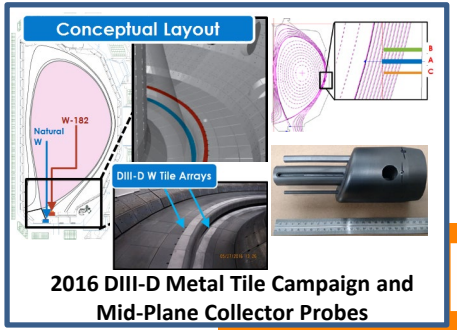

2016 DIII-D Metal Tile Campaign and Mid-Plane Collector Probes

Nuclear Materials and New Fusion Technology Courses Developed

- **NE 440** – Introduction to Nuclear Fuels and Materials (Zinkle, Fall) (PhD Qualifying Exam Material)
- **NE 460** – Introduction to Fusion Technology (Donovan, Fall)
- **NE 540** – Fundamentals of Irradiation Effects in Nuclear Materials (Zinkle/Lang, Spring) (PhD Qualifying Exam Material)
- **NE 563** – Boundary Plasma Physics and Plasma-Material Interactions (Donovan, Spring)
- **NE 660** – Defect Physics in Materials Exposed to Extreme Environments (Zinkle)
- **NE 661** – Gas Dynamics in Nuclear Materials (Wirth)
- **NE 662** – Advanced Characterization Methods Applied to Nuclear Materials (Lang)
- **NE 663** – Diagnostics for Plasma Physics and Fusion Technology (Donovan)

ITER is near, but significant fusion technology challenges remain

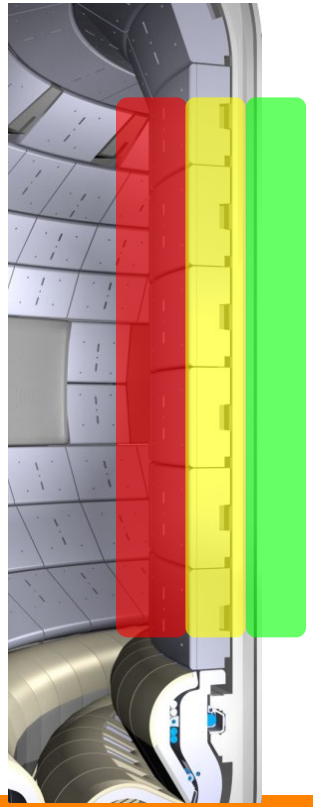

- **Plasma-Surface Interactions** (PSI) are among the most significant fusion technology issues that must be confronted.
- My work in PSI can be organized into three categories:

1. Plasma Boundary
   - Plasma sheath physics
   - Particle and heat flux approaching inner wall, Impurity Transport
2. Inner Wall Surface
   - Surface morphology changes due to bombardment from He ions and hydrides
   - Fuel trapping in inner wall material
3. Tritium Permeation through Inner Wall

Outline

- **What is a Scrape-Off Layer (SOL)?**
- **What is a Simple SOL?**
- **Explain why we don't want a Simple SOL, we actually want a Complex SOL**
- **What is a Complex SOL?**
- **Impurity transport in the SOL**
  - Check out PDF of slides to see hidden content with more details.

Source: Stangeby, *The Plasma Boundary of Magnetic Fusion Devices*, Taylor & Francis, 2000

Stangeby, *Plasma Boundary*, Chapter 1

Simple Analytic Models of the SOL

- Solid Surfaces are Sinks for Plasmas
- Tokamak: Example of a Low Pressure Gas Discharge Tube
- Tokamak Magnetic Fields
- Scrape-Off Layer
- Characteristic SOL Time
- 1D Fluid Approximation for the SOL Plasma
- Simple SOL and Ionization in the Main Plasma
- 1D Plasma Flow Along the Simple SOL to a Surface
- Comparison of the Simple SOL and Complex SOL

Source: Stangeby, *The Plasma Boundary of Magnetic Fusion Devices*, Taylor & Francis, 2000

Tokamak Magnetic Fields

- Tokamak *B* field made of toroidal field (B_φ) and poloidal field (B_θ).
  - B_φ typically created using external magnets.
  - B_θ created by toroidal plasma current (I_p) induced by external transformer.
- Resulting B_{total} is helical.
- Field lines combine to create a magnetic flux surface.
- Flux surfaces do not cross each other, they are nested inside of each other.
- *Closed* field lines do not intercept a solid surface.
- *Open* field lines do pass through a solid surface.

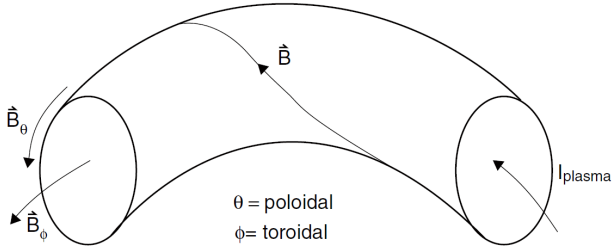

Figure 1.5: Toroidal direction is long way around, poloidal direction is short way around.

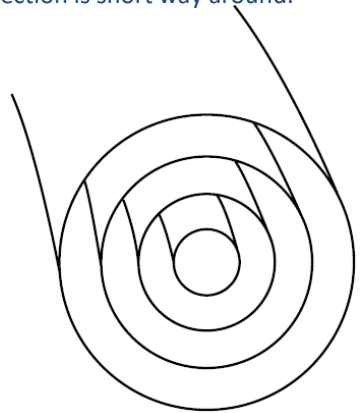

Figure 1.6: Magnetic flux surfaces forming set of nested toroids.

Source: Stangeby, *The Plasma Boundary of Magnetic Fusion Devices*, Taylor & Francis, 2000

What is the Scrape-Off Layer (SOL)?

- *Last closed flux surface (LCFS)*: going outwards from the main plasma, the last flux surface that does not touch a solid surface.
- All flux surfaces beyond the *LCFS* are open.
- SOL exists beyond the LCFS.

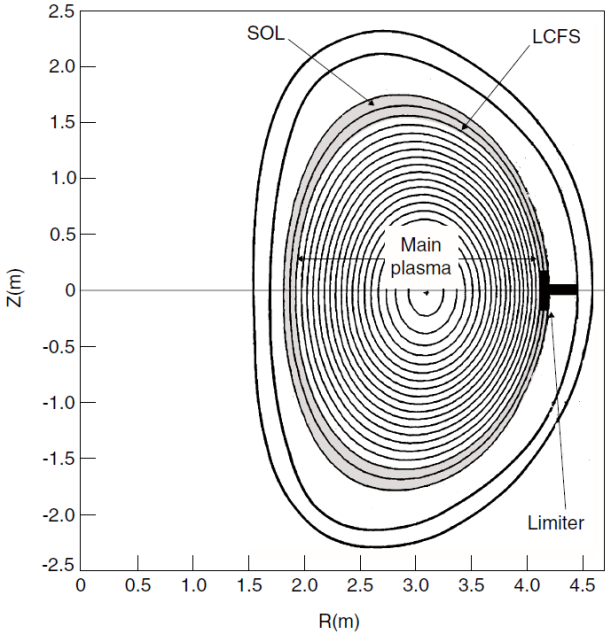

Figure 1.7: Limiter configuration.

Source: Stangeby, *The Plasma Boundary of Magnetic Fusion Devices*, Taylor & Francis, 2000

Safety Factor (q) is the # of toroidal transits required for B_{total} to make one poloidal transit

- Most magnetic field lines never close on themselves, eventually mapping out the entire flux surface.
- Resonance exists if the *safety factor* takes on a rational value for a given flux surface.
  - $q \approx \frac{rB_\varphi}{RB_\theta}$
  - Approximation for large *aspect ratio*, circular cross-section tokamak.
  - *Aspect Ratio* = *R/a*
  - *R* = major radius
  - *a* = minor radius of circular LCFS
  - *r* = minor radius of any given circular flux surface

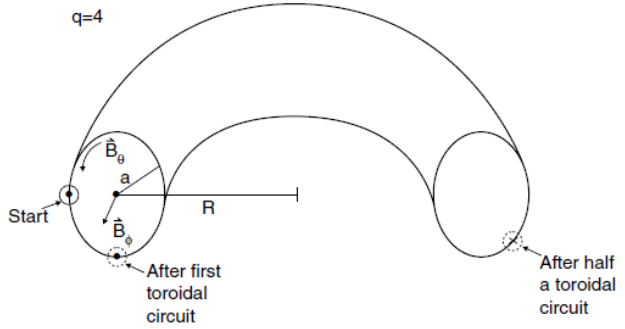

Figure 1.8. The safety factor q, when an integer, is the number of *toroidal* transits required for B_{total} to make one *poloidal* transit. The example shown is for $q = 4$.

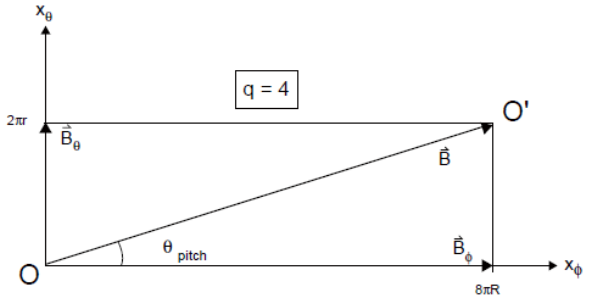

Figure 1.9. A single toroidal flux surface has been cut and flattened. The specific example of $q = 4$ is illustrated, showing that four toroidal transits are required for one poloidal transit.

Source: Stangeby, *The Plasma Boundary of Magnetic Fusion Devices*, Taylor & Francis, 2000

Safety Factor (q)

- q = 4 for a given flux surface means a field line takes 4 toroidal transits to complete one poloidal transit.
- $B_\theta(a) \approx \frac{\mu_0 I_p}{2\pi a}$
- q is large for small I_p and/or large B_φ.
- *Local Pitch Angle* of B_{total}.
  - $\theta_{pitch} \approx \frac{B_\theta}{B_\varphi} \approx \frac{B_\theta}{B}$
- $\theta_{pitch} \approx 0.1$ because tokamak magnetic field is primarily toroidal.
- Plasma more likely to experience MHD instabilities if $q \leq 2$ at the LCFS.

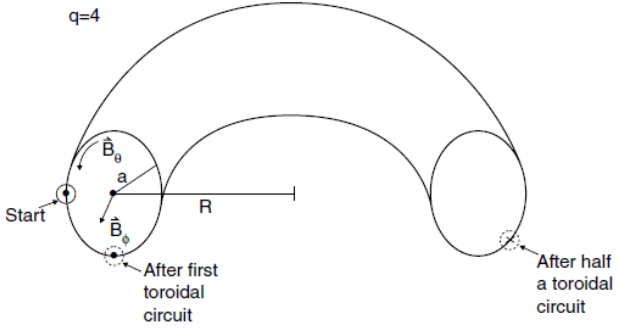

Figure 1.8. The safety factor q, when an integer, is the number of *toroidal* transits required for B_{total} to make one *poloidal* transit. The example shown is for $q = 4$.

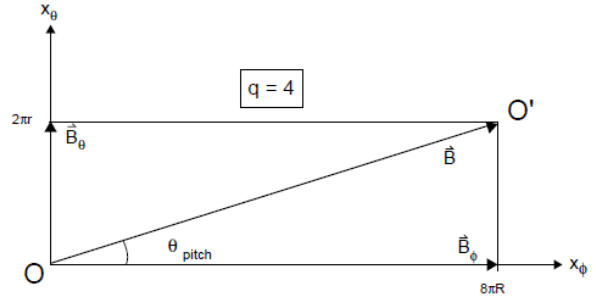

Figure 1.9. A single toroidal flux surface has been cut and flattened. The specific example of $q = 4$ is illustrated, showing that four toroidal transits are required for one poloidal transit.

Source: Stangeby, *The Plasma Boundary of Magnetic Fusion Devices*, Taylor & Francis, 2000

SOL transport consists of motion parallel and perpendicular to the *B*-field

- Cross-field velocities in SOL approximately:
  - $v_\perp \cong D_\perp / l_\perp$
  - $D_\perp$ = cross-field diffusion coefficient [m^2 sec^{-1}]
  - $l_\perp$ = characteristic radial scale length of density [m]
- Fick's Law: $\Gamma = -D\frac{dn}{dx}$
  - Γ = particle flux density [particles m^{-2} sec^{-1}]
  - *D* = particle diffusion coefficient
  - $\mathrm{d}n/\mathrm{d}x \approx n/l_\perp$
- $D_\perp$ is difficult to calculate from first principles, typically only able to be measured experimentally.
- $l_\perp$ is typically on the order of the ionization mfp of the recycling neutrals at the edge.
- $v_\parallel \approx c_s = \left[\frac{k(T_e+T_i)}{m_e+m_i}\right]^{1/2} \approx \left[\frac{k(T_e+T_i)}{m_i}\right]^{1/2}$
- **$v_\parallel$ typically orders of magnitude larger than $v_\perp$ causing SOL to be very thin relative to its length.**

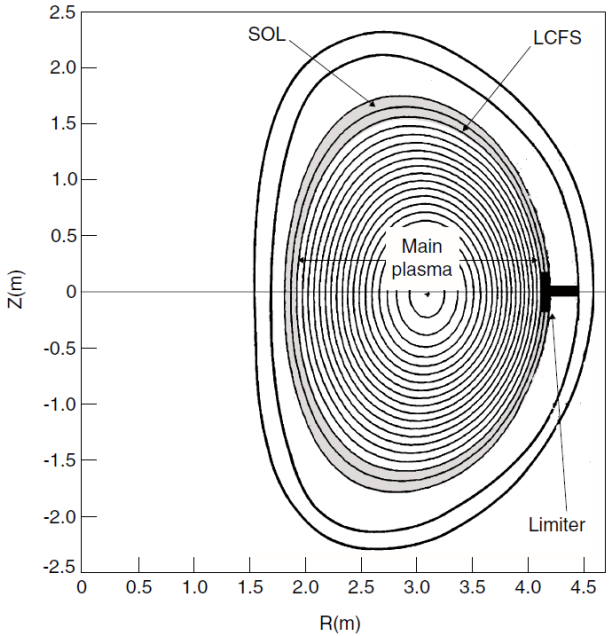

Figure 1.7: Limiter configuration.

Source: Stangeby, *The Plasma Boundary of Magnetic Fusion Devices*, Taylor & Francis, 2000

Limiter SOL

- *Poloidal Limiter*: annulus with inner radius *a* capable of producing almost perfectly circular LCFS.
- $L \approx \pi R/n$
  - Typical parallel-to-*B* distance a particle has to travel in the SOL before striking a limiter.
  - *n* = # of poloidal limiters
  - *L* = connection length
  - Distance along *B* in the SOL between two points of contact with the solid surface = 2*L*

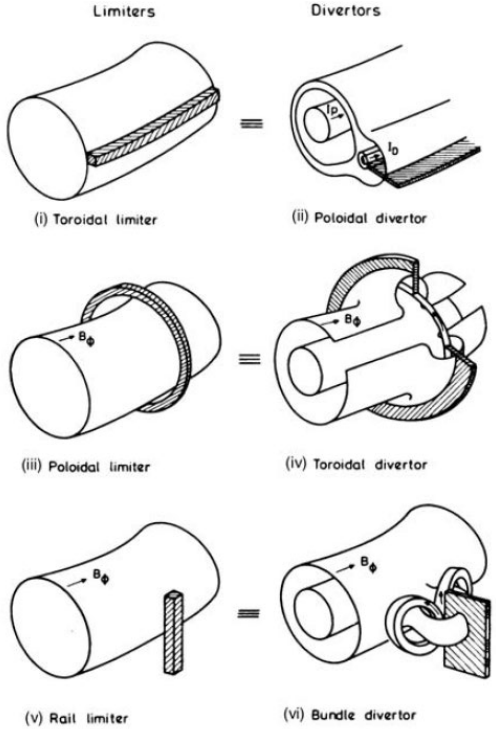

Figure 1.10. Various limiter and divertor configurations [1.37]:

Source: Stangeby, *The Plasma Boundary of Magnetic Fusion Devices*, Taylor & Francis, 2000

Most early tokamaks used limiters to control plasma shaping

- *Toroidal Limiter*: full toroidal circular rail, typically at mid-plane.
- Connection Length: $L \approx \pi R q$
  - Much longer *L* due to small pitch angle of *B*.
  - L > 100 m in large tokamaks like JET.
  - SOL radial width still only ~1 cm due to large $v_{\parallel}/v_{\perp}$
- Any shape of object inserted into the plasma can act as a limiter (*Rail Limiter).*
- *Wall Limiter* simply uses the inner wall (typically near the mid-plane) as the limiter.
  - Often increases the *plasma-wetted area* and lowers peak heat flux.

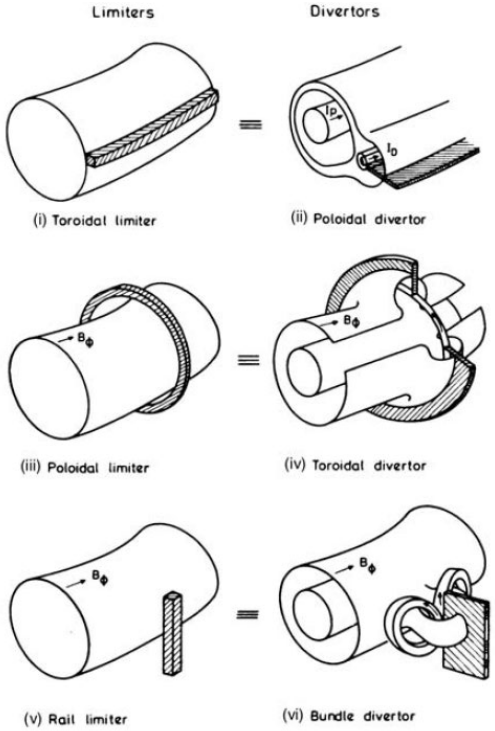

Figure 1.10. Various limiter and divertor configurations [1.37]:

Source: Stangeby, *The Plasma Boundary of Magnetic Fusion Devices*, Taylor & Francis, 2000

Divertor configurations began taking over in the 1980's

- *Limiter tokamaks* rely primarily on I_p to create circular poloidal *B* fields.
- *Poloidal divertor* produced using an external conductor carrying current I_D in the same direction as I_p.

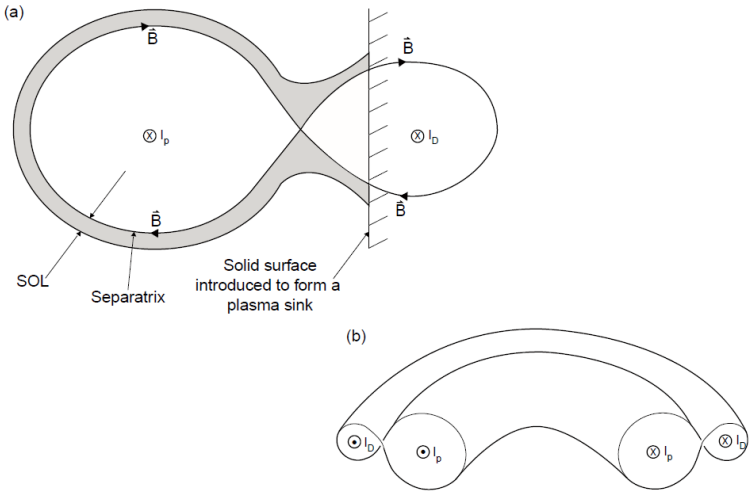

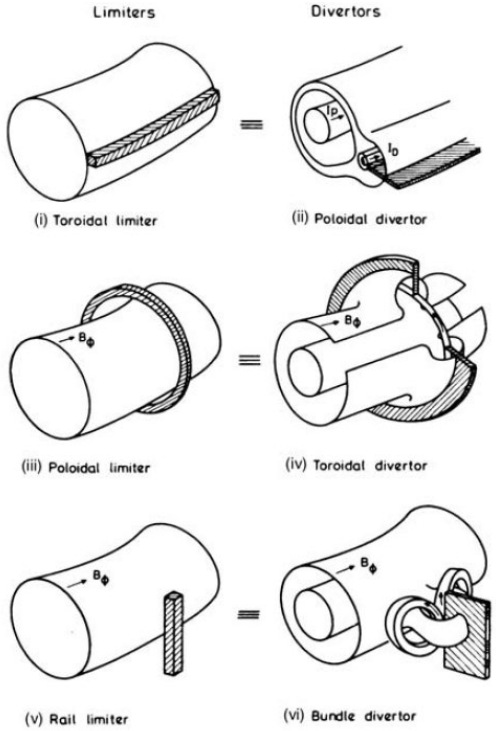

Figure 1.10. Various limiter and divertor configurations [1.37]:

Figure 1.11. The poloidal field B_θ^{plasma} created by I_{plasma} is *diverted* by the B_θ^{coil} created by a *divertor coil* current I_D, parallel to I_{plasma}, which is carried by a coil internal or external to the vacuum vessel.

Source: Stangeby, *The Plasma Boundary of Magnetic Fusion Devices*, Taylor & Francis, 2000

Divertor operation moved the target out of direct contact with the main plasma

- *X-point* created at the null between the two current centers.
- *Separatrix* is the magnetic flux surface passing through the X-point and creates the LCFS.
- Inside the separatrix is the *main* or *confined plasma* within closed flux surfaces.
- *Divertor Target*: solid surface intersecting the magnetic flux surfaces created by I_D.
- Particles that cross the separatrix move rapidly to the divertor target before diffusing very far cross-field.

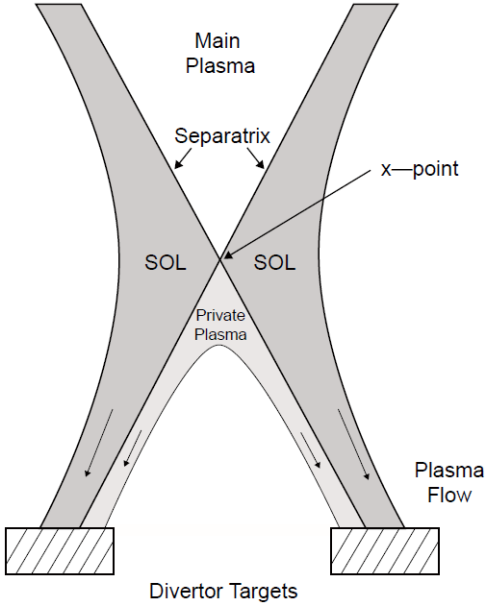

Figure 1.12: The SOL surrounds the main plasma above the X-point and extends to the target. The private plasma receives particles and energy from the SOL by cross-field transport.

Source: Stangeby, *The Plasma Boundary of Magnetic Fusion Devices*, Taylor & Francis, 2000

Divertor SOL

- If target is not far from X-point (short ‘divertor legs’), length of average SOL field line is similar to limiter configuration:
  - $L \approx \pi R q$
  - Short legs are good because it reduces overall confined volume (reduces costs for magnets and vessel).
- In principle, field line on the separatrix is infinite in length.
- In reality, *magnetic shear* near the separatrix can cause ‘shorting’ of long field lines on to adjacent shorter field lines.
- *L* at the separatrix is typically quoted as the value immediately outside the separatrix.
- *Private Plasma*: region below the X-point and inside the separatrix.
  - Very thin layer of plasma adjacent to the divertor legs.
  - Plasma sustained by transport of particles and power from the main SOL across the private plasma separatrix.
- Divertor configuration is less efficient in the use of magnetic volume than limiters.
- Divertors have been found to be far more beneficial than limiters for overall confinement and reduction of plasma impurities.

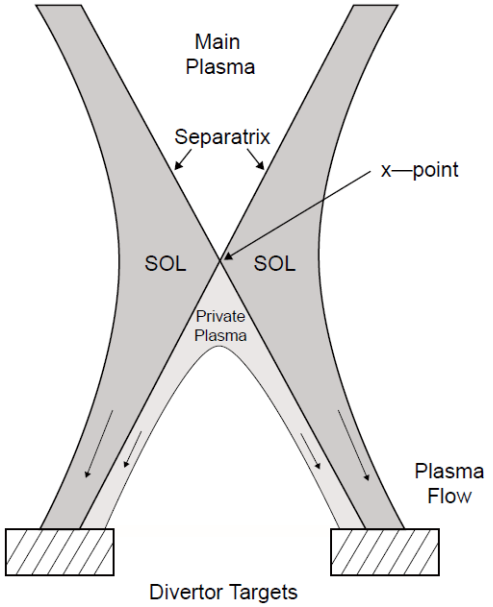

Figure 1.12: The SOL surrounds the main plasma above the X-point and extends to the target. The private plasma receives particles and energy from the SOL by cross-field transport.

Source: Stangeby, *The Plasma Boundary of Magnetic Fusion Devices*, Taylor & Francis, 2000

Average SOL dwell time is around 100-1000x shorter than average Main Plasma dwell time

- *Poloidal Divertor* and *Toroidal Limiter* are most common operating configurations.
  - Large *plasma-wetted areas*.
  - $L \approx \pi R q$
  - Plasma particles moving parallel-to-*B* in the SOL have velocities ≈ plasma sound speed (c_s).
- Characteristic particle dwell times in the SOL:
  - $\tau_{sol} \cong L/c_s$
- Typical edge parameters:
  - $kT \approx$ 1-100 eV
  - $c_s \approx 10^4 - 10^5$ m/sec
  - JET: $R \approx 3$ m; $q = 4$; $L \approx 40$ m
  - Result $\tau_{sol} \approx 1$ msec
  - Characteristic dwell time in main plasma ≈ 1 sec

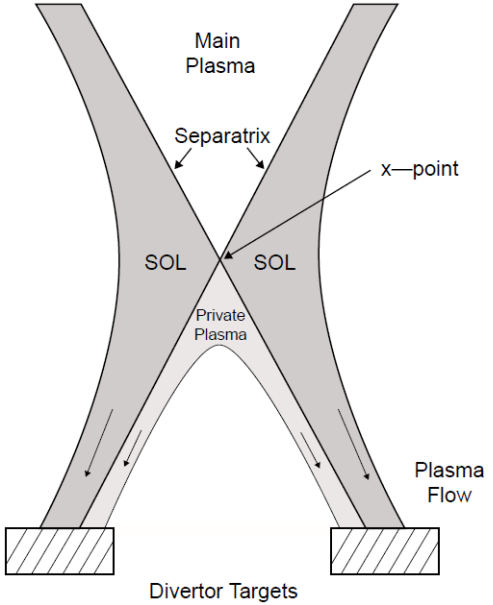

Figure 1.12: The SOL surrounds the main plasma above the X-point and extends to the target. The private plasma receives particles and energy from the SOL by cross-field transport.

Source: Stangeby, *The Plasma Boundary of Magnetic Fusion Devices*, Taylor & Francis, 2000

1D Fluid Approximation for the SOL Plasma

- *1D approximation* ignores toroidal magnetic curvature.
- *Neo-classical effects* that arise from 'toroidicity' (non-zero value of *a/R*) are ignored.
- SOL is 'straightened out' and analyzed either 1D or 2D.

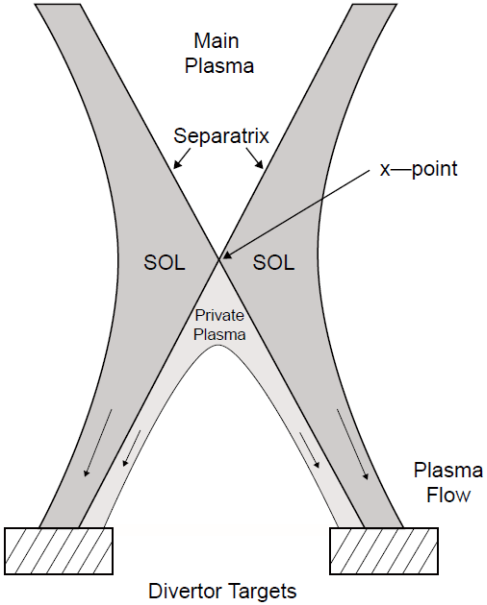

Figure 1.12: The SOL surrounds the main plasma above the X-point and extends to the target. The private plasma receives particles and energy from the SOL by cross-field transport.

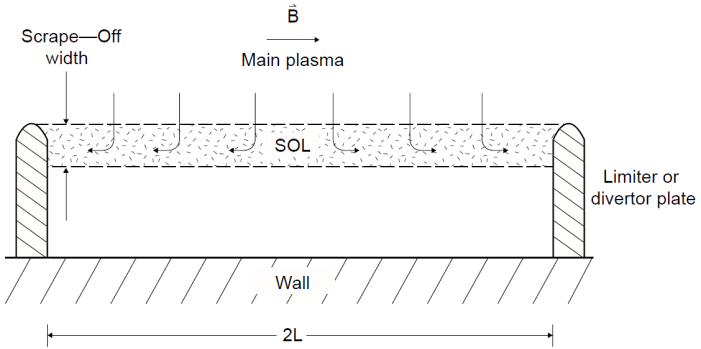

Figure 1.13. The SOL has been straightened out. Energy and particles flow from the main plasma into the SOL by slow cross-field transport, followed by rapid transport parallel to ***B*** along the SOL to the targets.

Source: Stangeby, *The Plasma Boundary of Magnetic Fusion Devices*, Taylor & Francis, 2000

1D Fluid Approximation for the SOL Plasma

- Rationale for ignoring neo-classical effects is due to relatively high level of collisionality in the colder plasma of the SOL.
- Self-collisional mfp are approximately:
  - $\lambda_{ee} \approx \lambda_{ii} \approx 10^{16} T^2 / n_e$
- **SOL is *collisional* if $\lambda < L$.**

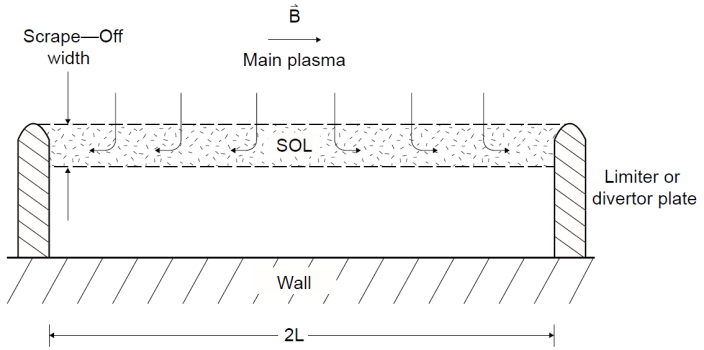

Figure 1.13. The SOL has been straightened out. Energy and particles flow from the main plasma into the SOL by slow cross-field transport, followed by rapid transport parallel to $\boldsymbol{B}$ along the SOL to the targets.

Table 1.1. Representative SOL conditions.

	JET	CMOD
T_e [eV]	50	10
n_e [m^{-3}]	10^{19}	10^{20}
L [m]	40	8
ν_e^*	25	1000
$\lambda_{ee}, \lambda_{ii}$ [m]	2.5	0.01
$\tau_{SOL} = L/c_s$ [ms]	0.6	0.3

Stangeby, *The Plasma Boundary of Magnetic Fusion Devices*, Taylor & Francis, 2000

Fluid vs. Kinetic analysis for plasma transport

- *Fluid analysis* is used for highly collisional plasmas.
  - Uses an average value of various quantities at each point in space and time.
- *Kinetic analysis* is used for more collisionless plasmas.
  - Complete *velocity distribution* (x,y,z,v_x,v_y,v_z,t) is needed at every point in space and time.
- *Fluid approximation* is typically appropriate for the SOL and is most often used.
  - Conditions in SOL can still often be marginal as to collisionality regime and requires further analysis.
- 2D SOL analysis assumes toroidal symmetry, resulting in two situations:
  - Radially cross-field and along *B* (top figure)
  - Radial and poloidal projection of the motion along *B* (bottom figures)
- Basic interpretive analysis largely relies on 1D analytic modeling (along *B*) and treats cross-field transport as sources of particles and energy.

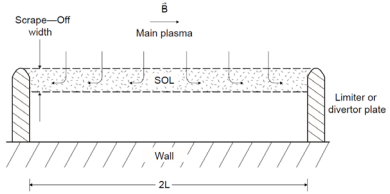

Figure 1.13. The SOL has been straightened out. Energy and particles flow from the main plasma into the SOL by slow cross-field transport, followed by rapid transport parallel to ***B*** along the SOL to the targets.

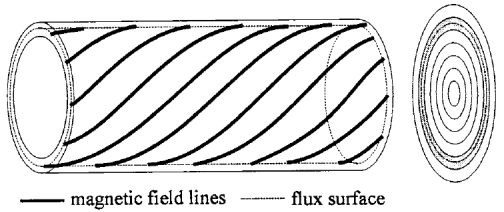

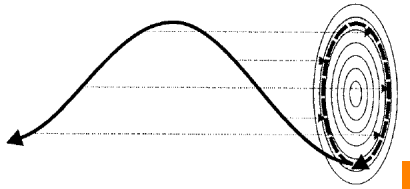

Figure 1.14. The path of a magnetic field line projected onto a poloidal plane. Distances along the field line $s_\parallel$ have corresponding value in the poloidal plane, s_θ. Analysis of the plasma behaviour can then be calculated in terms of $s_\parallel$ or s_θ.

Source: Stangeby, *The Plasma Boundary of Magnetic Fusion Devices*, Taylor & Francis, 2000

Simple SOL assumes all ionization is in the Main Plasma

- *Simplest assumption*: recycled neutrals have sufficiently long mfp to pass through the SOL and ionize in the main plasma.
- More likely in *limiter* configuration because recycling surface is in contact with the main plasma.
- Recycled neutrals reach main plasma, ionize, eventually diffuse back out into SOL to act as a roughly uniform source of ions into SOL.
- Plasma particles diffuse cross-field beyond the LCFS a characteristic distance:
  - $\lambda_{SOL} \cong (D_\perp \tau_{SOL})^{\frac{1}{2}} = (D_\perp L/c_s)^{1/2}$
  - λ_{SOL} typically a few cm.

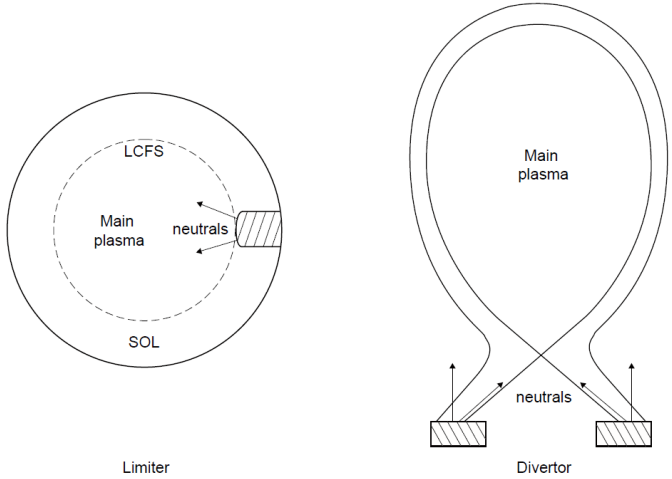

Figure 1.15. Neutral hydrogen recycling from a limiter tends to be ionized inside the LCFS, while hydrogen recycling from divertor targets tends to be ionized in the SOL and private plasma.

Source: Stangeby, *The Plasma Boundary of Magnetic Fusion Devices*, Taylor & Francis, 2000

Complex SOL allows for ionization in the SOL

- *Simple SOL* assumes the only source of ions is from the main plasma.
- *Complex SOL* involves ionization in the SOL as well as the main plasma.
  - Ionization in the SOL is typically not good because it reduces particles reaching the main plasma.
  - SOL ionization is often a significant fraction of total ionization of recycled neutrals.
- Previous equation for λ_{SOL} only valid for simple SOL.

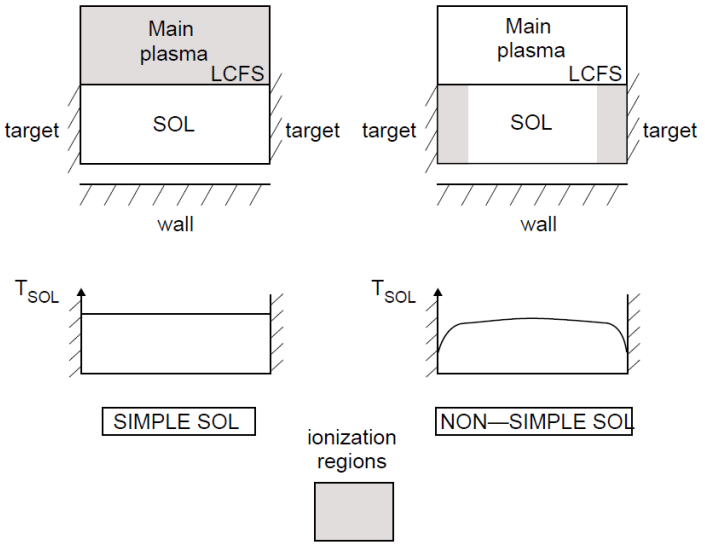

Figure 1.16. For the simple SOL, ionization occurs in the main plasma and the temperature is constant along a given SOL flux tube. For the non-simple SOL, the ionization usually occurs in the SOL and near the targets; also the SOL temperature drops approaching the target, along each SOL flux tube.

Source: Stangeby, *The Plasma Boundary of Magnetic Fusion Devices*, Taylor & Francis, 2000

Beveling of surfaces result in larger area for heat deposition and reduction of peak heat flux

- Small values of λ_{SOL} result in small *plasma-wetted areas (A_{wet})*.
- Results in excessive peak heat flux.
- Beveling of limiting surface can greatly increase A_{wet}.
- Poloidal divertors, A_{wet} can be increased by increasing the radial separation of the poloidal magnetic flux surfaces using external magnetic fields.

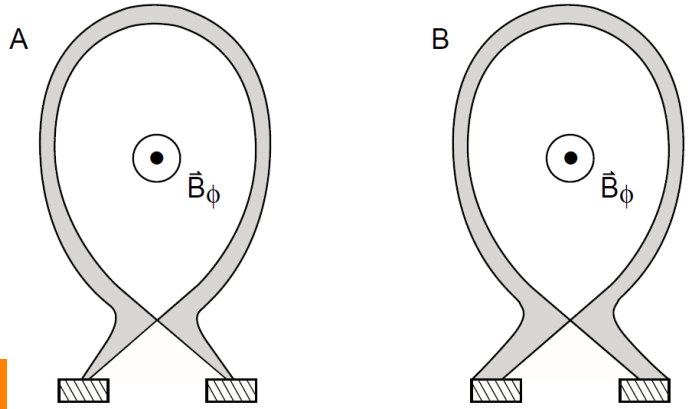

Figure 1.19. The divertor plasma can be spread over a larger target area, case B, compared with case A, by expanding the poloidal field at the targets, i.e., by making B_θ weaker there.

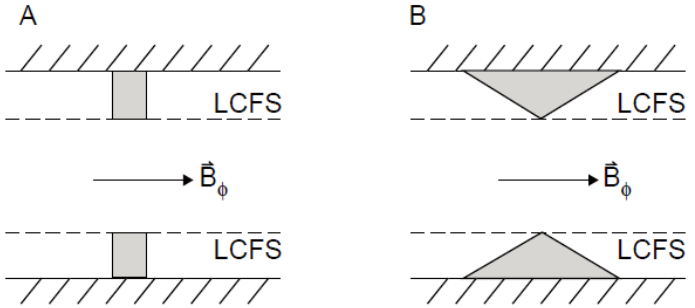

Figure 1.17. The bevel-sided poloidal limiter B has a larger plasma-wetted area than the flat-sided A. Toroidal view.

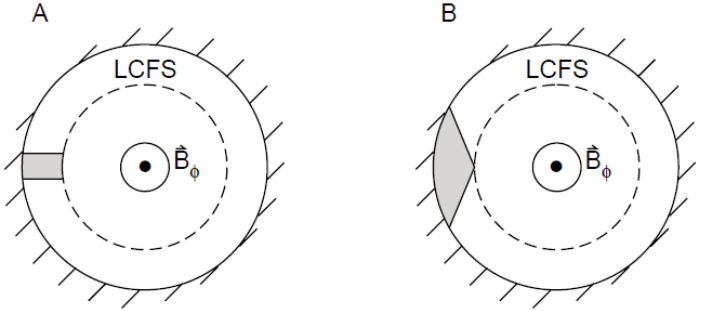

Figure 1.18. The bevel-sided toroidal limiter B has a larger plasma-wetted area that the flat-sided A. View of the poloidal cross-section.

Stangeby, *The Plasma Boundary of Magnetic Fusion Devices*, Taylor & Francis, 2000

Source: Stangeby, *The Plasma Boundary of Magnetic Fusion Devices*, Taylor & Francis, 2000

1D Plasma Flow Along the Simple SOL to a Surface – Basic Features

1) Parallel pressure gradient induced in the SOL plasma by the presence of a source and sink drives plasma flow.
   - *Total* pressure is constant along *B*
   - *Static* pressure decreases, providing the force.
   - $p_{total} = p_{static} + p_{dynamic}$
   - $p_{dynamic} = mnv^2$ = *flux of flow momentum*
   - As p_{static} decrease, $p_{dynamic}$ (as well as *v*) increases.

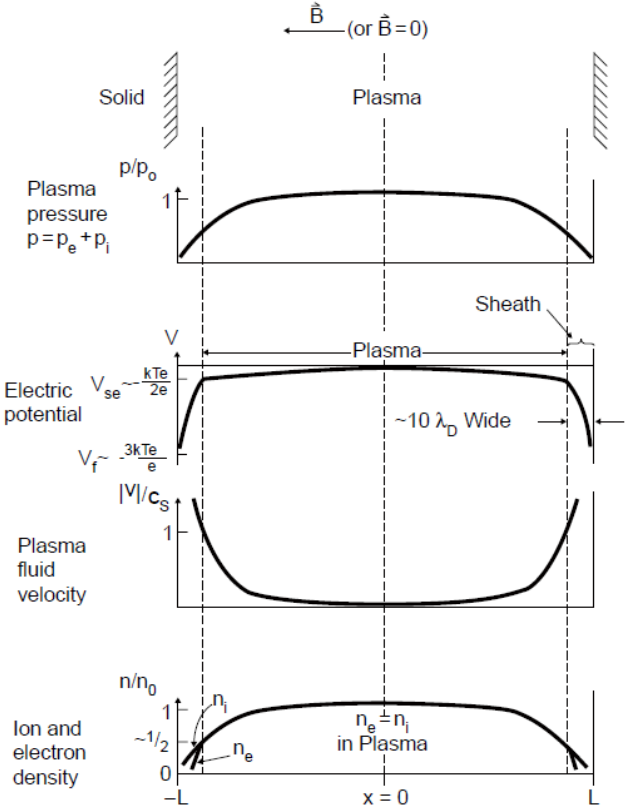

Figure 1.20. Schematic of the variation of plasma pressure, electric potential, plasma velocity and ion/electron densities in the plasma between two semi-infinite planes. The thickness of the sheath is exaggerated for clarity. The total length is $2L$.

Source: Stangeby, *The Plasma Boundary of Magnetic Fusion Devices*, Taylor & Francis, 2000

1D Plasma Flow Along the Simple SOL to a Surface – Basic Features

2) e^- charge up solid surface negatively within μs of plasma startup.

- Small mass and high velocity of e^- compared to ions allows them to reach the walls far quicker.

3) Negatively charged walls slow e^- loss rate and increase ion loss rate.

- Floating surface, potential adjusts until loss rates of ions and e^- are equal, known as *ambipolar* plasma transport.
- Creates an *ambipolar electric field* in the plasma.
- Solid surfaces charge to a potential of $V_{wall} \sim -3kT_e/e$ for a hydrogenic plasma relative to *plasma potential.*
- Plasma is an excellent conductor parallel to *B,* so potential is nearly constant along any given *B* field line.

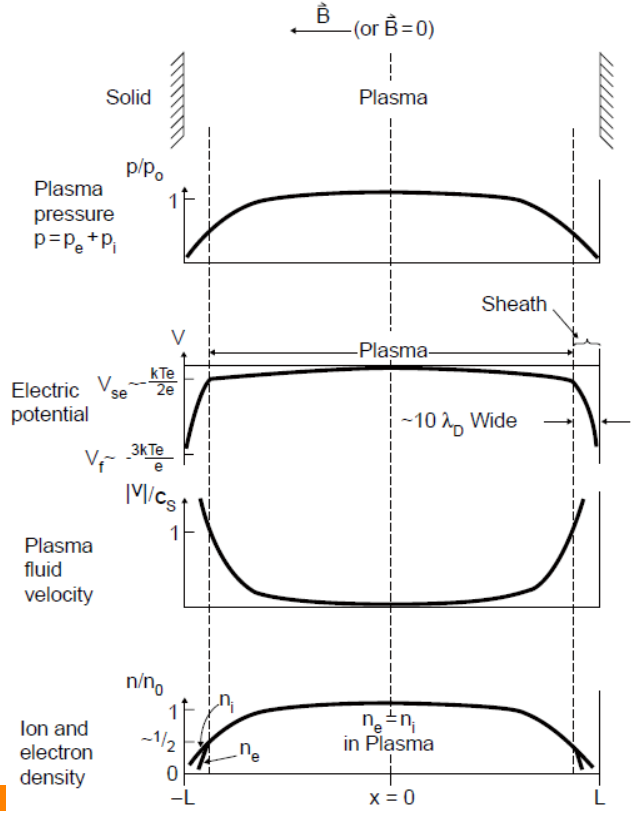

Figure 1.20. Schematic of the variation of plasma pressure, electric potential, plasma velocity and ion/electron densities in the plasma between two semi-infinite planes. The thickness of the sheath is exaggerated for clarity. The total length is $2L$.

Source: Stangeby, *The Plasma Boundary of Magnetic Fusion Devices*, Taylor & Francis, 2000

1D Plasma Flow Along the Simple SOL to a Surface – Basic Features

4) *Debye shielding* almost entirely shields the plasma from electrostatic potentials on surfaces (floating or applied bias) within a small distance (*Debye length*).
   - $\lambda_{Debye} = \left(\frac{\varepsilon_0 k T_e}{n_e e^2}\right)^{1/2}$
   - T_e = 20 eV, $n_e = 10^{19}$ m^{-3}, $\lambda_D \approx 10^{-5}$ m
   - *Debye sheath* is region of net positive space charge in dynamic equilibrium.
   - Ions continue to move through sheath at high speed.
   - Positive charge density [C/m^2] integrated over sheath thickness ≈ negative charge density on solid surface.
5) Shielding is imperfect and small electric field penetrates the length of the plasma to the source.
   - *Pre-sheath electric field*: $E \approx kT_e/2eL$
   - Acts on the ions in the SOL to help move them toward the target.

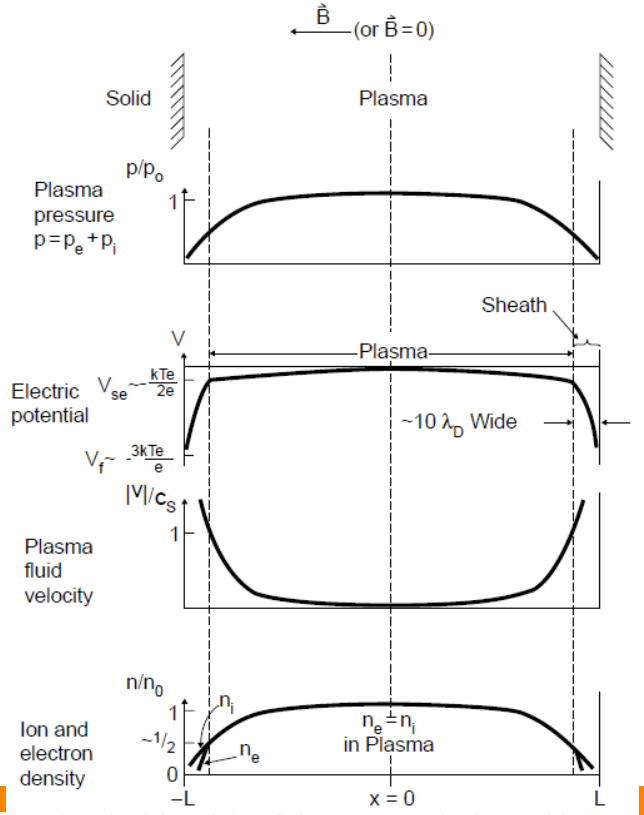

Figure 1.20. Schematic of the variation of plasma pressure, electric potential, plasma velocity and ion/electron densities in the plasma between two semi-infinite planes. The thickness of the sheath is exaggerated for clarity. The total length is $2L$.

Source: Stangeby, *The Plasma Boundary of Magnetic Fusion Devices*, Taylor & Francis, 2000

1D Plasma Flow Along the Simple SOL to a Surface – Basic Features

6) Surface sink action causes a drop in local plasma density creating *parallel density and pressure gradient.*
   - Pre-sheath creates momentum/force balance between:
     - Parallel pressure gradient force pushing e^- towards surface.
     - Retarding *E* field force pushing away from surface.
   - e^- obey *Boltzman factor* relation:
     - $n = n_0 e^{eV/kT_e}$
     - n_0 = upstream plasma density where $V \approx 0$
     - *V* becomes more negative approaching surface.

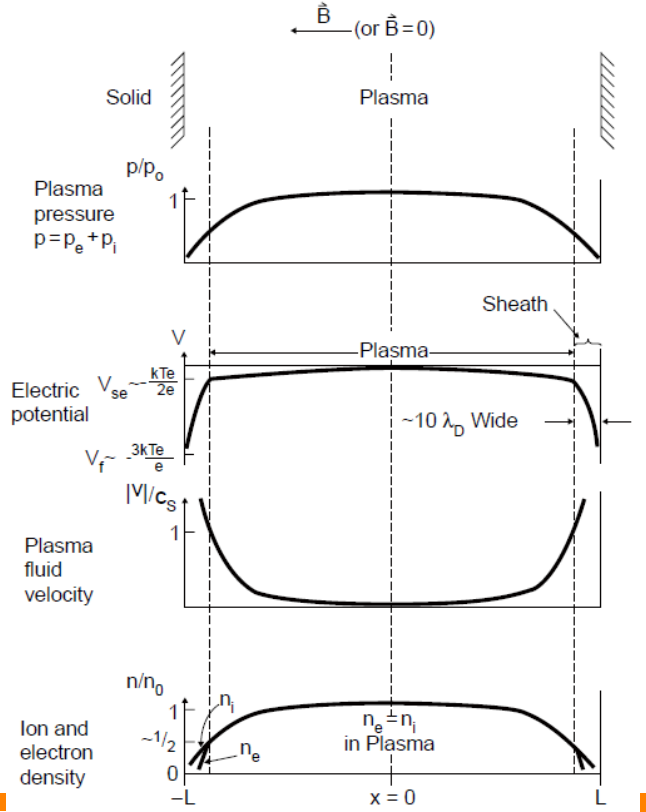

Figure 1.20. Schematic of the variation of plasma pressure, electric potential, plasma velocity and ion/electron densities in the plasma between two semi-infinite planes. The thickness of the sheath is exaggerated for clarity. The total length is $2L$.

Source: Stangeby, *The Plasma Boundary of Magnetic Fusion Devices*, Taylor & Francis, 2000

1D Plasma Flow Along the Simple SOL to a Surface – Basic Features

7) Ambipolar *E* field does not exert a net force on the combined *plasma* fluid.
   - Acts on both ion and e^- fluids individually.
   - Net effect from *E* field cancels out.
   - Only accelerating force towards the surface is from the pressure gradient.

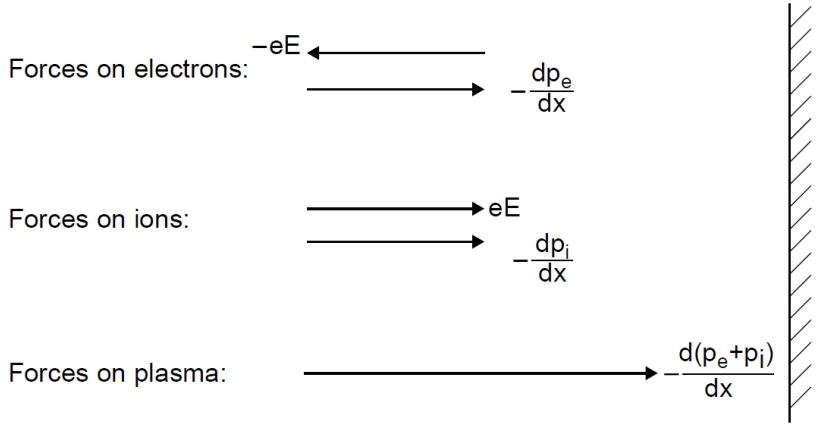

Figure 1.21. The electrons are almost in perfect force balance, while for the ions the electric field force and the ion pressure gradient force are additive (and equal if $T_e = T_i$, the case shown here), accelerating the ions. The force on the plasma is due to the total pressure gradient alone, since an electric field exerts no force on the quasineutral plasma.

Source: Stangeby, *The Plasma Boundary of Magnetic Fusion Devices*, Taylor & Francis, 2000

1D Plasma Flow Along the Simple SOL to a Surface – Basic Features

8) Plasma is *isothermal* along any given flux tube in the SOL.
   - Result of very high heat conductivity along the tube.
   - A definition of a *simple SOL* is small parallel *T*-gradients, constituting *sheath-limited regime*.
   - Fluid speed of both charge species at the sheath edge (v_{se}) is the ion acoustic speed (c_s).
     - $c_s = \left[\frac{k(T_e+T_i)}{m_i}\right]^{1/2}$
9) Plasma density drops from n_0 at distance L upstream to $n_{se} = \frac{1}{2}n_0$ at sheath edge.

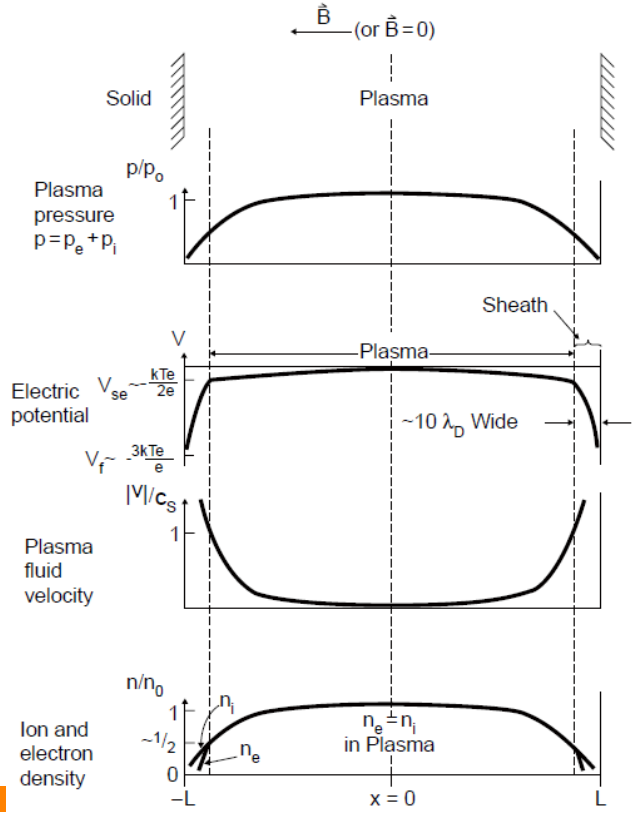

Figure 1.20. Schematic of the variation of plasma pressure, electric potential, plasma velocity and ion/electron densities in the plasma between two semi-infinite planes. The thickness of the sheath is exaggerated for clarity. The total length is $2L$.

Source: Stangeby, *The Plasma Boundary of Magnetic Fusion Devices*, Taylor & Francis, 2000

1D Fluid Equations

- *Particle Flux Density*: $\Gamma = nv$ = [particles m^{-2} sec^{-1}]
  - v = fluid speed (not individual particle speed that has a random thermal component)
- Conservation of particles (mass) in 1D steady-state:
  - $(\Gamma_{out} - \Gamma_{in})A = \left(\Gamma_{in} + \Delta x \frac{d\Gamma}{dx} - \Gamma_{in}\right)A = \Delta x A \frac{d\Gamma}{dx} = \Delta x A S_p$
  - S_p = particle source = [particles m^{-3} sec^{-1}]
  - $\frac{d\Gamma}{dx} = \frac{d(nv)}{dx} = S_p$
- Newton's 2nd Law:
  - $F = ma = m\frac{dv}{dt} = m\frac{dv}{dx}\frac{dx}{dt} = mv\frac{dv}{dx}$
- Applied to n particles per m^3 and summing relevant fluid forces:
  - $nF = neE - \frac{dp}{dx} - nF_{drag}$
  - neE = parallel E-force exerted on particles of charge $+e$

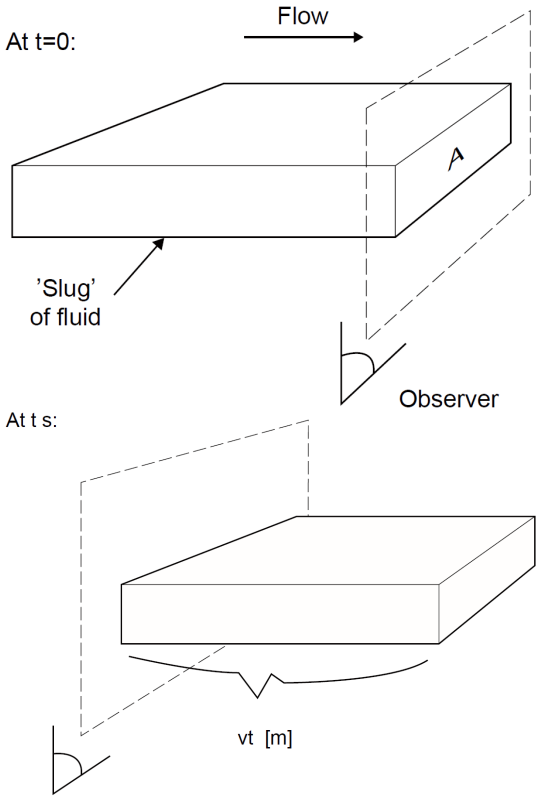

Figure 1.22. Demonstration that $\Gamma = nv$.

Source: Stangeby, *The Plasma Boundary of Magnetic Fusion Devices*, Taylor & Francis, 2000

1D Fluid Equations

- Net pressure force:
  - $\left[-\left(p+\Delta x\frac{dp}{dx}\right)+p\right]A=-\Delta xA\frac{dp}{dx}$
- Most drag forces ignored (viscous, collisions).
- Drag force from S_p is included.
  - Newly ionized particles assumed to start stationary and must be accelerated to bulk fluid velocity, creating net drag on bulk momentum.
- 1D SS Momentum Eqn:
  - $nmv\frac{dv}{dx}=neE-\frac{dp}{dx}-mvS_p$
- Plasma assumed to be isothermal, so energy conservation equation not needed.
- Two equations, two unknowns: *n(x), v(x)*
  - Because isothermal, *T* is a parameter not a variable, so pressure is found from *n* and *v*.
  - $p(x)=kTn(x)$
  - If not isothermal, Cons. of Energy eqn. needed to find third variable, *T(x)*.
- Boltzmann relation allows us to remove *E* as a dependent variable a well.

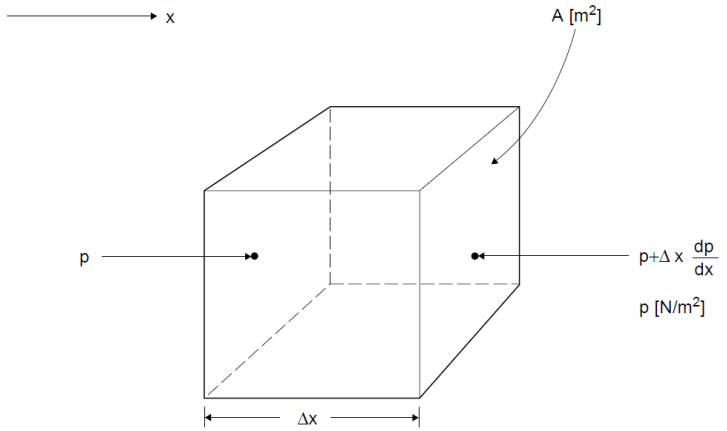

Figure 1.24. Demonstration of the pressure-gradient force.

Source: Stangeby, *The Plasma Boundary of Magnetic Fusion Devices*, Taylor & Francis, 2000

Boltzmann Relation for Electrons

- Momentum Equation for electron fluid:
  - $nm_e v\frac{dv}{dx} = -neE - \frac{dp_e}{dx} - m_e v S_p$
- Assume *L* is characteristic parallel length of spatial variations along the SOL.
- Cons. Of Particles: $S_p = \frac{d(nv)}{dx} \approx \frac{nv}{L}$
  - $nm_e v\frac{v}{L} \approx -neE - n\frac{kT_e}{L} - m_e v\frac{nv}{L}$
- Assume drift speed along SOL is c_s:
  - $nm_e\frac{c_s^2}{L} = -neE - \frac{nkT_e}{L} - \frac{m_e nc_s^2}{L}$
- Assume isothermal ($T_i = T_e$)
  - $n\frac{m_e}{m_i}\frac{2kT}{L} \approx -neE - \frac{nkT}{L} - n\frac{m_e}{m_i}\frac{2kT}{L}$
- m_e/m_i << 1 means inertia term and drag term are insignificant compared to pressure gradient term.
- Force balance for electrons is between the *E*-field ($E \equiv -\mathrm{d}V/\mathrm{d}x$)and the pressure gradient (-dp_e/d*x*).
- Integrating over *x* gives the Boltzmann relation: $n = n_0 e^{eV/kT_e}$

Source: Stangeby, *The Plasma Boundary of Magnetic Fusion Devices*, Taylor & Francis, 2000

Modelling the Ions

- Modelling e^- in the SOL is easier because they very closely obey the Boltzmann relation and typically maintain a Maxwellian velocity distribution.
- Ions are accelerated in the SOL, perturbing their velocity distribution to potentially become non-Maxwellian.
- Particle Cons: $\frac{d(nv)}{dx} = S_p$
- Momentum Cons: $nmv\frac{dv}{dx} = -\frac{dp_i}{dx} + enE - mvS_p$
- Assume: singly charged ions; $n_e = n_i$; Ambipolar flow ($v_e = v_i$); $S_{pe} = S_{pi}$
- Assume isothermal: $\frac{dp_i}{dx} = kT_i\frac{dn}{dx}$
- Boltzmann for e^- provides E: $enE = -kT_e\frac{dn}{dx}$
- *Plasma* Momentum Eqn combines ion and electron eqns and assuming $m = m_e + m_i$:
  - $nmv\frac{dv}{dx} = -mc_s^2\frac{dn}{dx} - mvS_p$
  - Sum of ion and electron pressure gradient forces.
  - *enE* component cancels out when summing ions and electrons.
- *Plasma Mach Number:* $M \equiv v/c_s$
- Combine Particle Cons. and Plasma Momentum Eqns:
  - $\frac{dM}{dx} = \frac{S_p}{nc_s}\frac{(1+M^2)}{(1-M^2)}$

Source: Stangeby, *The Plasma Boundary of Magnetic Fusion Devices*, Taylor & Francis, 2000

Ionization Rate Coefficient Calculations

- Monte Carlo computer codes written to incorporate multiple ionization reactions including DEGAS, EIRENE, NIMBUS.
- Modeling of the neutrals is being coupled to 2D SOL fluid codes (B2, UEDGE, EDGE2D).
- For simplicity, assume effective ionization rate is an average of reactions 1 and 6.
- Ionization particle source rate:
  - $S_{p,iz} = n n_n \overline{\sigma v_{iz}}(T_e)$ [ion pairs m^{-3} sec^{-1}]
  - n = plasma density (strictly n_e)
  - n_n = neutral density (average of atomic and molecular)

Figure 1.25. The rate coefficients for atomic and molecular hydrogen [1.23]. The numbered reactions are (1): $e + H_2 \rightarrow H_2^+ + 2e$, (2): $e + H_2 \rightarrow 2H^0 + e$, (3): $e + H_2 \rightarrow H^0 + H^+ + 2e$, (4): $e + H_2^+ \rightarrow 2H^0$, (5): $e + H_2^+ \rightarrow H^0 + H^+ + e$, (6): $e + H^0 \rightarrow H^+ + 2e$, and charge exchange (7): $H^0 + H^+ \rightarrow H^+ + H^0$.

Source: Stangeby, *The Plasma Boundary of Magnetic Fusion Devices*, Taylor & Francis, 2000

‘Source’ of plasma into Simple SOL is cross-field diffusion from the Main Plasma

- *Radial,* cross-field direction *r*, perpendicular to B_{SOL}.
- Parallel (relative to *B* field in SOL) removal to the solid surface is particle *sink* for cross-field particle flux density ($\Gamma_\perp$).
- Cons. of Particles:
  - $\frac{d\Gamma_\perp}{dr} = S_{p\perp} < 0$
- Cross-field sink gives parallel source term ($S_{p,c\text{-}f}$):
  - $S_{p,c-f} \equiv S_{p\parallel} = -S_{p\perp}$
- Assume $\Gamma_\perp$ obeys Fick’s law of diffusion:
  - $\Gamma_\perp = -D_\perp \frac{dn}{dr}$
- Plasma decays radially with characteristic length λ_{SOL}:
  - $\frac{dn}{dr} \cong -\frac{n}{\lambda_{SOL}} \Rightarrow \frac{d^2n}{dr^2} \cong \frac{n}{\lambda_{SOL}^2}$
- $S_{p,c-f} = D_\perp n/\lambda_{SOL}^2$

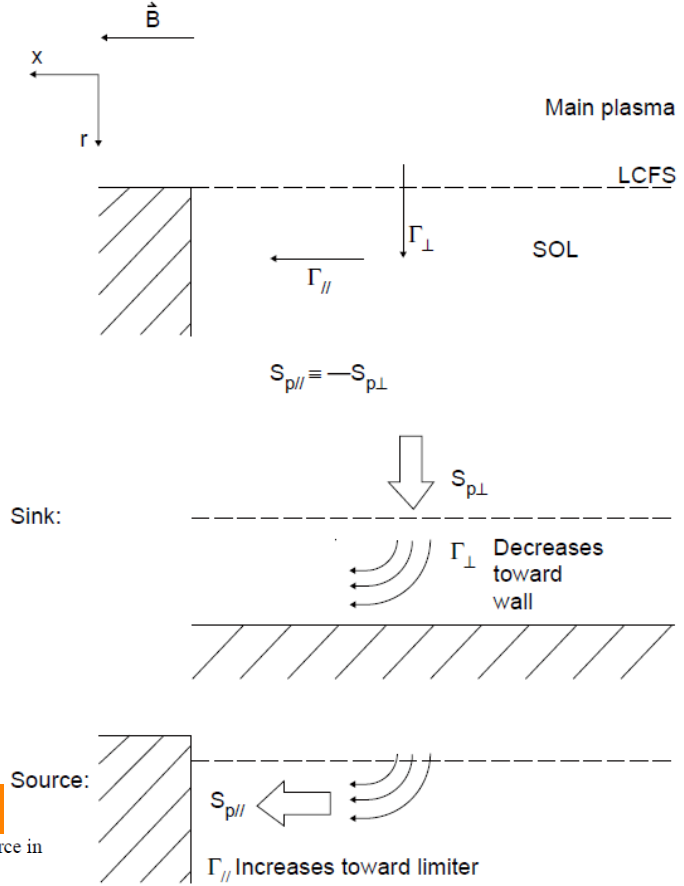

Figure 1.32. Cross-field diffusion into the SOL constitutes an effective particle source in 1D, along-the-SOL modelling.

Source: Stangeby, *The Plasma Boundary of Magnetic Fusion Devices*, Taylor & Francis, 2000

Sonic Flow of Isothermal Plasma into the Sheath

- Recall from ion modelling: $\frac{dM}{dx} = \frac{S_p}{nc_s}\frac{(1+M^2)}{(1-M^2)}$
  - *Plasma Mach Number:* $M \equiv v/c_s$
  - *Sonic flow*: velocity approaches sound speed ($v = c_s$), so $M = 1$.
- Note S_p/nc_s is intrinsically positive.
- Assume flow is stagnant ($v(0) = M(0) = 0$) a distance of L from the surface (halfway between surfaces).
- $dM/dx > 0$ at x = 0 with flow accelerating towards the surface.
- $M \to 1$ results in dM/dx approaching infinity and would imply infinite gradients for n, v, V.
- We want to assume M approaches 1 at the plasma-sheath interface, so we accept that all gradients become infinite at the plasma-sheath interface.

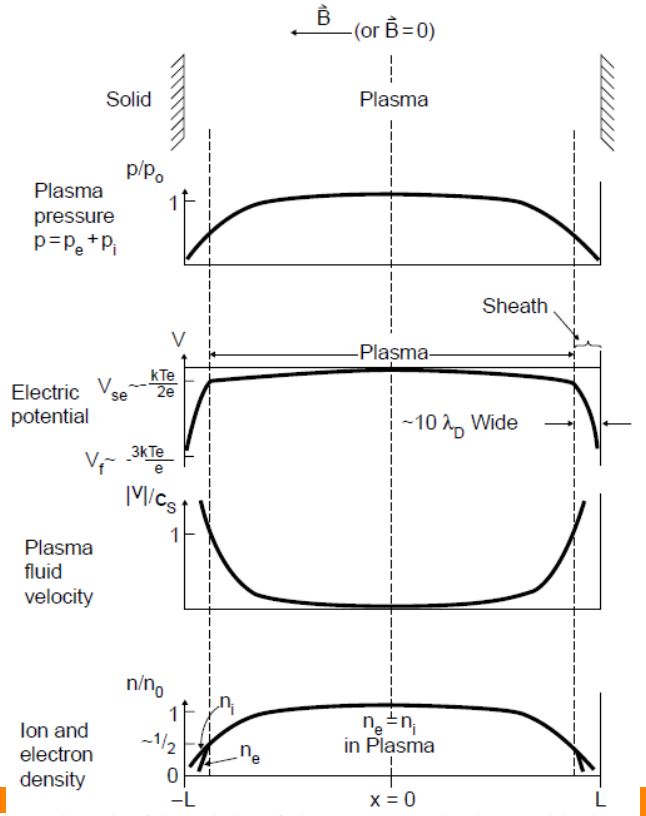

Figure 1.20. Schematic of the variation of plasma pressure, electric potential, plasma velocity and ion/electron densities in the plasma between two semi-infinite planes. The thickness of the sheath is exaggerated for clarity. The total length is $2L$.

Source: Stangeby, *The Plasma Boundary of Magnetic Fusion Devices*, Taylor & Francis, 2000

Sonic Flow of Isothermal Plasma into the Sheath

- Section 2.3 demonstrates how we can assume $M \approx 1$ at the plasma-sheath interface by analyzing from the *sheath* side using the *Bohm criterion.*
- Fluid subject to an uncompensated pressure difference of order $\Delta p \approx p$ will 'explode'.
  - Particles accelerated to near c_s in the direction of the Δp force.
- Combine ion and e^- momentum equations to give plasma fluid equation for a freely expanding, no-source, 1D fluid:
  - $nmv\frac{dv}{dx} = -\frac{dp}{dx}$
  - $p \equiv p_e + p_i$
- Plasma only experiences Δp force in direction along B.
- Sheath acts as a perfect sink for ions causing Δp along flow direction $\approx p$.
  - $\frac{mnv^2}{L} \approx \frac{p}{L} \approx \frac{nkT}{L}$
  - L is gradient scale length, v is representative velocity.
- Results in formula for free expansion of a fluid at the sound speed *(c_s):*
  - $v \approx (kT/m_i)^{1/2}$

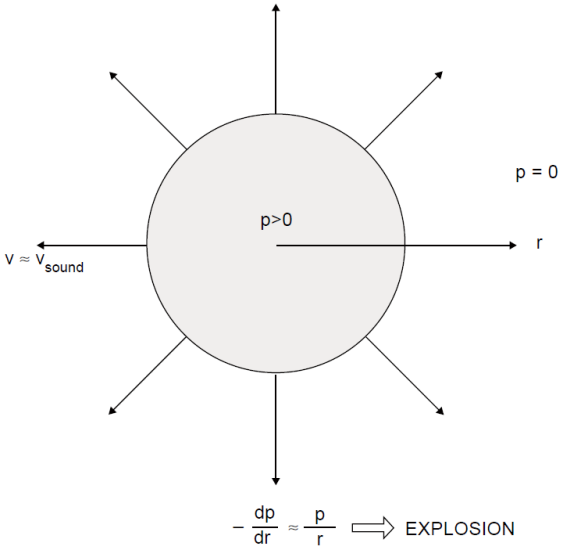

Figure 1.33. An uncompensated pressure-gradient force of magnitude $-\mathrm{d}p/\mathrm{d}r \simeq p/r$ causes a fluid to expand explosively rapidly.

Source: Stangeby, *The Plasma Boundary of Magnetic Fusion Devices*, Taylor & Francis, 2000

Velocity Distribution Along the SOL

- For $S_{p,iz}$ or $S_{p,c\text{-}f}$, define: $S_p = Cn$
  - C is a positive parameter whose value is yet to be determined.
- Recall from ion modelling: $\frac{dM}{dx} = \frac{S_p}{nc_s}\frac{(1+M^2)}{(1-M^2)}$
  - $\int_0^M \frac{1-M^2}{1+M^2} dM = \int_0^x \frac{C dx}{c_s}$
  - $2\tan^{-1} M - M = \frac{Cx}{c_s}$
- Introduce boundary condition: $M(L) = 1$
  - Actually should be at $L - \lambda_{Debye}$, but we assume λ_{Debye} is small compared to L.
- Already assumed $M(0) = 0$
- $\frac{\pi}{2} - 1 = \frac{CL}{c_s}$
  - Indicates source strength is constrained by space available (L) and plasma temperature (c_s).
  - C, L, c_s must balance for the plasma to be steady-state.

Source: Stangeby, *The Plasma Boundary of Magnetic Fusion Devices*, Taylor & Francis, 2000

Variation of Plasma Density Along the SOL

- *Conservative form of the momentum equation* obtained from algebraic manipulation of two conservation equations:
  - $\frac{d}{dx}(p_e + p_i + mnv^2) = 0$
  - $p_e + p_i + mnv^2 = \text{constant}$
- For isothermal assumption:
  - $n(x) = \frac{n_0}{1+[M(x)]^2}$ where $n_0 = n(0)$
  - General form for density, independent of S_p and its spatial variations.
  - Recall we know $M(x)$: $(2\tan^{-1} M - M = \frac{Cx}{c_s})$
  - So $n(x)$ can now be found.
  - $n(x)$ only drops by a factor of ~2 from upstream to edge for isothermal conditions.
- *Particle flux density at sheath edge:* $\Gamma_{se} = \frac{1}{2} n_0 c_s$

Source: Stangeby, *The Plasma Boundary of Magnetic Fusion Devices*, Taylor & Francis, 2000

Average Dwell-Time in the SOL, τ_{SOL}

- Flow velocity is not constant along the SOL, so we assume $v \approx \frac{1}{2}\, c_s$ for spatially 'well-distributed' sources.
- Two methods of estimating τ_{SOL} that have already been discussed:
  - $\tau_{SOL} \approx \frac{L}{c_s}$
  - $\tau_{SOL} = \frac{\bar{n}_{SOL} L}{\frac{1}{2} n_0 c_s} \approx \frac{L}{c_s}$
    - Think of τ_{SOL} as particle confinement time in SOL, so particle content of the SOL is divided by particle outflux.
- Once again, calculation of τ_{SOL} for a *Complex SOL* is more complicated because *n(x)* varies much more over the SOL.

Source: Stangeby, *The Plasma Boundary of Magnetic Fusion Devices*, Taylor & Francis, 2000

Parallel Electric Field in the SOL

- Boltzmann Equation: $n = n_0 e^{eV/kT_e}$
- $n(x) = \frac{n_0}{1+[M(x)]^2}$
- Combine to eliminate *n*:
  - $V(x) = -\frac{kT_e}{e}\ln[1 + (M(x))^2]$
- *M(x)* has already been defined, giving us *V(x)* and $E_{\|}(x)$ (pre-sheath *E* field).
- At the sheath edge:
  - $V_{se} \equiv V(L) = \frac{kT_e}{e}\ln 2 \cong -0.7\frac{kT_e}{e}$
- Any larger potential applied externally to a plasma is shielded by the Debye sheath.
- Spontaneous wall charging for floating (*ambipolar*) conditions results in negative surface potential of ~-3kT_e/e for H plasmas.
  - Surface potential appears across the sheath while only ~-0.7kT_e/e penetrates into the plasma.
  - Constitutes the ambipolar *E* field needed to move ions through the SOL to the sink (Section 2.6).

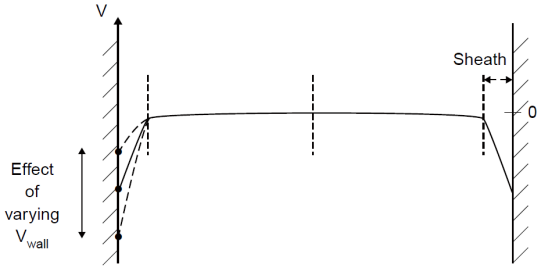

Figure 1.36. Variation of the electric potential on a wall or an electrode is almost entirely 'soaked up' within the thin sheath, leaving the plasma unaffected. Here the potential on the 'far' (right) wall is assumed not to change as the potential of the 'near' (left) wall is varied relative to the plasma potential, which is taken to be $V = 0$ here. See section 2.6 for the case where a potential difference is applied between the two end walls.

Source: Stangeby, *The Plasma Boundary of Magnetic Fusion Devices*, Taylor & Francis, 2000

Validity of Isothermal Fluid Assumption for the SOL

- Isothermal fluid assumption neglects:
  - Natural cooling of a flow as it accelerates to sonic speed.
  - Self-collisional mfp can often be $\geq L$, invalidating fluid treatments.
  - Viscous effects have been ignored.
- Comparisons with more sophisticated models (see hidden slides) including above effects have not shown appreciable difference, so this model is valid for the *Simple SOL*.
- Does *NOT* account for **parallel temperature gradients**.
  - Arise in the SOL due to finite parallel heat conductivity of the edge plasma.
  - Results in the *Conduction-Limited Regime*, which is very important for divertor tokamaks.
  - Parallel ion temperature gradient caused by acceleration of the flow.
  - Converts static pressure into dynamic pressure.

Source: Stangeby, *The Plasma Boundary of Magnetic Fusion Devices*, Taylor & Francis, 2000

Comparison of Various SOL Models

Table 1.2. Calculated sheath related quantities from various models. $T_e = T_i$.

Quantity	Normal-ization factor	Model							
		1	2	3	4	5	6	7	Ave
1. Plasma density at sheath edge, n_{se}	n_0	0.50	0.40	0.60	0.52	0.50	0.50	0.43	0.51
2. Plasma flow velocity at sheath edge, v_{se}	$(2kT_0/m_i)^{1/2}$	1.00	1.13	0.95	0.90	1.05	1.03	0.88	0.99
3. Normalized potential at sheath edge, η_{se}	kT_0/e	−0.69	−0.72	−0.41	−0.65	−0.69	−0.69	−0.86	−0.67
4. Normalized (floating) wall potential, η_w	kT_0/e	−3.19	−3.08	−2.91	−3.26	−3.13	−3.15	−3.45	−3.17
5. Particle outflux density, Γ_{se}	$n_0(2kT_0/m_i)^{1/2}$	0.50	0.55	0.63	0.47	0.53	0.52	0.38	0.51

Models.

1. Isothermal fluid model, section 10.2 [1.32].
2. Adiabatic fluid model [1.32].
3. Kinetic model of Emmert *et al*., section 10.7 [1.33].
4. Kinetic model of Bissell *et al*., section 10.7[1.34].
5. Fluid, collisionless model, $T_\perp^i \neq T_\parallel^i$, section 10.8 [1.35].
6. Fluid, collisional model, $T_\perp^i = T_\parallel^i$, section 10.9 [1.35].
7. Kinetic model with cross-field viscosity, $\eta_\perp = nmD_\perp$ [1.36].

In order to make a valid comparison, the results of [1.33–1.35] were used for $T_e = T_\perp^i(0) = T_\parallel^i(0) \equiv T_0$, temperature at the symmetry point of the system (e.g., at $x = 0$ of a SOL, figure 1.20), rather than for the examples actually illustrated in [1.35], where $T_\parallel^i(0) < T_\perp^i(0)$; H^+ ions; no secondary electron emission; see chapter 10 for a more complete discussion of these comparisons.

Source: Stangeby, *The Plasma Boundary of Magnetic Fusion Devices*, Taylor & Francis, 2000

Simple SOL vs. Complex SOL

- Most important SOL property is whether there is a *significant temperature drop along the length of the SOL*.
- *Sheath-Limited Regime*: plasma is nearly isothermal along each individual flux tube.
  - Sheath is the only important driver of power/particles in the edge plasma from inside the separatrix to the solid surface.
- *Conduction-Limited Regime*: significant parallel temperature drop between upstream location ($x = 0$) and sheath-edge in front of the target.
  - Plasmas have finite heat conductivity that can be significant for long L (true for many divertor configurations).
  - Classical conductivity varies as $T^{5/2}$ and temperature in the SOL is much cooler than the core.

Source: Stangeby, *The Plasma Boundary of Magnetic Fusion Devices*, Taylor & Francis, 2000

Simple SOL vs. Complex SOL

- SOL *plasma density* and *temperature* are 'limited' by the regime, rather than *power* (escapes regardless of regime).
- Level of ionization in the SOL is also important.
- *Simple SOL* is *sheath-limited* and also does not have local ionization.
- *Complex SOL* is typically *conduction-limited* and can have local ionization and other complicating features.

Table 1.3. The principal distinctions between simple and complex SOLs.

		Simple SOLs	Complex SOLs
1.	Parallel temperature gradients	$\nabla_{\parallel} T_{e,i} \approx 0$	$\nabla_{\parallel} T_{e,i} \neq 0$
2.	Thermal coupling of electrons and ions	de-coupled	coupled
3.	Particle source	cross-field transport from the main plasma	ionization within the SOL is important
4.	Volumetric sources and sinks of particles, momentum and energy in the SOL	none	can be important

Source: Stangeby, ***The Plasma Boundary of Magnetic Fusion Devices***, Taylor & Francis, 2000

What is possible for a Complex SOL?

1. Temperature gradients parallel to ***B***.
2. Ionization in the SOL of recycling neutral H.
3. Volume power loss in SOL due to radiation (H and impurities) and CX neutrals.
4. Momentum loss by the plasma flow to neutral H.
5. Volume recombination if *T* drops below a few eV.
6. Collisional transfer of energy between *e*- and ions.
7. Viscous drag.
8. Loss of particles/momentum/energy from SOL into private plasma.
    - Limiter SOL are usually Simple.
    - Divertor SOL are usually Complex.
    - Simple SOL is easier to analyze, but better performance is achieved for Complex SOL (divertor) conditions.

Source: Stangeby, *The Plasma Boundary of Magnetic Fusion Devices*, Taylor & Francis, 2000

Benefits of a Complex SOL

- Large *T* gradients often preferable.
  - Low *T* near the target reduces sputtering.
  - High *T* upstream near the LCFS allows for operating conditions with fewer instabilities.
    - For Simple SOL (no parallel *T* gradient), maintaining low *T* throughout the SOL requires high $\bar{n}_{main}$ for a given *P*.
- Ionization occurring primarily in the SOL as opposed to the Main Plasma results in more *heat conduction* and less *parallel heat convection*, allowing for a larger *T* gradient.
  - Simple SOL, ions only come from Main Plasma and enter ~uniformly along the LCFS.
  - Causes significant parallel plasma flow (and *parallel heat convection*) and greatly outweighs *parallel conduction*, thereby *decreasing the parallel drop in T*.

Source: Stangeby, *The Plasma Boundary of Magnetic Fusion Devices*, Taylor & Francis, 2000

Benefits of a Complex SOL

- Volume power losses in the SOL are good because they spread out the radiated heat flux over the larger wall area.
- Low *T* near the target also beneficial because recycling neutrals cause neutral frictional drag on the plasma flow to the targets.
  - *Neutral cushion* protects the target.
- For *T* at the target $\leq$1 eV, volume recombination is strong.
  - Replaces sink action of solid target with *gaseous target*, reducing target erosion and heating.

Source: Stangeby, *The Plasma Boundary of Magnetic Fusion Devices*, Taylor & Francis, 2000

Low T high n regimes at the target

- For low divertor target temperature (T_t), several types of beneficial operating regimes become possible (in order of decreasing T_t and increasing n_t):
  - *High Recycling*
  - *Strongly Radiating*
  - *Detached*
- For high n_t, ionization occurs close to the targets.

Source: Stangeby, *The Plasma Boundary of Magnetic Fusion Devices*, Taylor & Francis, 2000

High Recycling Regime

- As T_t drops, particle flux to the target (ϕ_t) has been found to *increase*.
  - For fully saturated solid surface, steady-state recycle fueling sets in.
  - Plasma sustains itself in terms of particles: plasma (ion) outflow (ϕ_t^+) = neutral inflow rate ($\phi_{neutral}^0$)
  - Low T_t regime is also a high recycling regime (high ϕ_t).
- Low T_t means sputtering yield is low.
- Unless volume power loss changes, power still reaches the target causing heat removal issues.
- *Conduction-limited regime* and *high recycling regime* often used interchangeably.
  - Both involve low T_t and large n_t.

Source: Stangeby, *The Plasma Boundary of Magnetic Fusion Devices*, Taylor & Francis, 2000

Strongly Radiating Regime

- *High Recycling* regime transitions into the *Strongly Radiating* regime as intensity of H recycling increases along with strong radiative losses.
- As T_e decreases, amount of radiative energy loss per recycling H and impurity atom increases.
  - At lower T_e, more excitations occur before ionization.
  - At very low T_e, recombination contributes to radiative power.
- *Strongly Radiating* regime can be reached for progressively lower T_e, particularly near the target.
- If radiating zone is too close to the target, then a significant fraction of the radiative power can still reach the target.

Figure 3.34. The atomic hydrogen electron cooling energy per ionization event, ε [eV/ionization] [3.48]. For $n_e = 10^{14}, 10^{16}, 10^{18}, 10^{20}, 10^{22}$ m^{-3} (the higher the value of n_e the lower the value of ε).

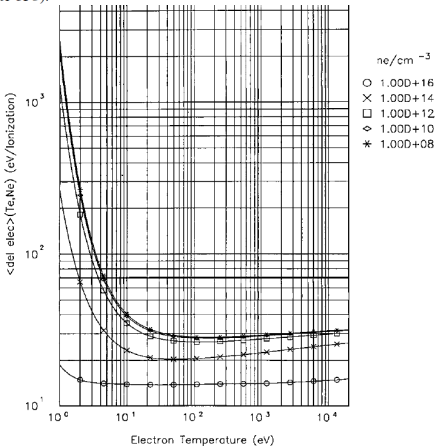

Figure 3.21. Radiative loss functions ('coronal equilibrium') for Be, B, C, Ne, Ar and Kr [3.46].

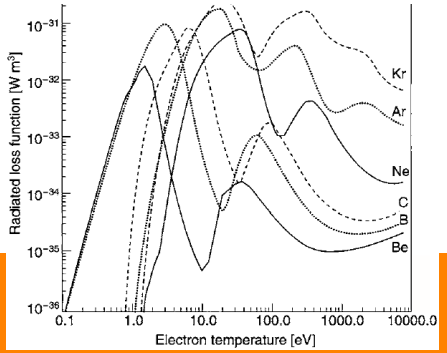

Source: Stangeby, *The Plasma Boundary of Magnetic Fusion Devices*, Taylor & Francis, 2000

These SOL regimes are easier to achieve with divertors rather than limiters

- *Detached Regime* occurs for the lowest T_t where both neutral friction drag and volume recombination are strong.
  - Detached divertor state characterized by very low n_t, T_t, Γ_t.
  - Much reduced target sputtering and heating.
- Limiter operation will always involve significant ionization in main plasma.
- Divertor operation allows targets to be located remotely such that nearly all ionization occurs in the SOL.
- Avoidance of significant ionization in the main plasma is required for the complex SOL.
- Figure shows location of H recycle ionization for limiter tokamaks.
  - Most ionization does not occur in the SOL.
  - For $n_{LCFS} > 10^{19}\ \mathrm{m}^{-3}$, higher ionization in SOL, but this is untypically high density for limiters.

Tokamak	Refs	Code	$\bar{n}_e$ ($10^{19}\mathrm{m}^{-3}$)	n_{LCFS} ($10^{18}\mathrm{m}^{-3}$)	Ionization fraction in SOL(%)
PLT (rail limiters)	Ruzic *et al* [4.39]	DEGAS	5.5	5	31
DITE (poloidal limiter)	Maddison *et al* [4.40]	DEGAS	2 2	5 2	14 7
JET (eight rail limiters)	Simonini *et al* [4.41]	NIMBUS	1.4 1.6 2.1 2.1 2.6 3.25 1.79 2.6 3.05 3.63 3.95	1.2 1.7 2.2 2.2 3.0 4.1 2.8 4.0 5.5 7.5 10	21 26 30 25 25 24 28 30 31 31 36
T-10	Pigarov and Vershkov [4.42]	TNG	2.6 (1.8)	4.5 (14.4)	43 63

[a] For ohmic heating; the two values in brackets are for ECH, electron cyclotron heating.

Table 4.1. Fraction of ionization occurring with the SOL of limiter tokamaks (using multi-dimensional neutral codes)[a].

Source: Stangeby, *The Plasma Boundary of Magnetic Fusion Devices*, Taylor & Francis, 2000

Additional Information

- "*The Plasma Boundary of Magnetic Fusion Devices*", Peter Stangeby, Taylor & Francis, 2000
  - First 6 chapters provide an excellent introduction to boundary plasma physics.
  - Primary text used in my PMI course at UTK.
- Feel free to e-mail me for additional lecture content (ddonovan@utk.edu).

Source: Stangeby, *The Plasma Boundary of Magnetic Fusion Devices*, Taylor & Francis, 2000

Collector probes combined with W isotopic tracer particles together create a first-of-its-kind global impurity transport diagnostic

- Impurity collector probes are used to assess impurity content in the Scrape-Off Layer (SOL).

1) Size of collector probes is used to control the sampling length upstream and downstream.

2) Ex-situ characterization of collector probe using RBS provides deposition profiles.

3) Isotopic tracer particles connect impurity production at the divertor to impurity transport in the SOL.

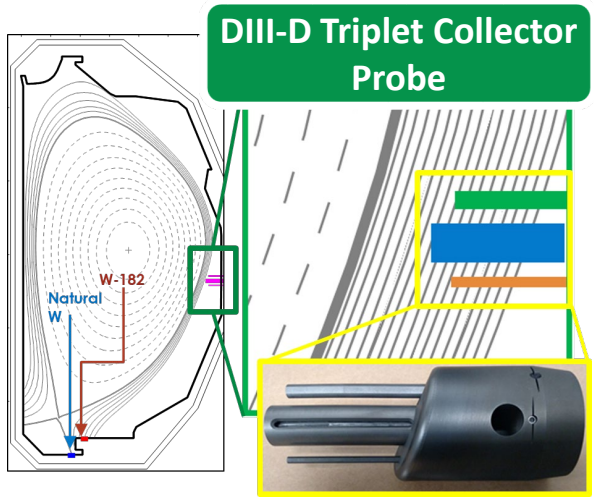

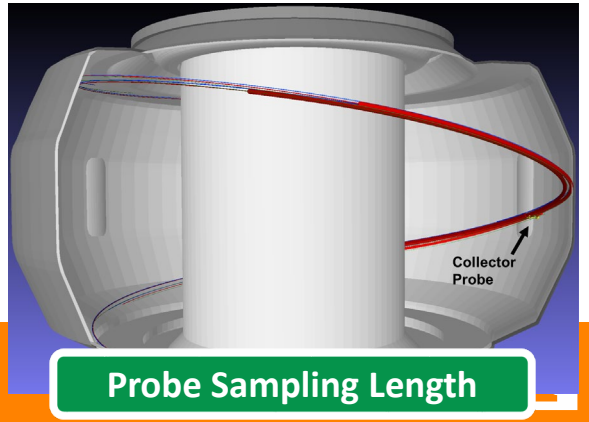

Basic Metrics Helped Define Main Measurements of Experiment

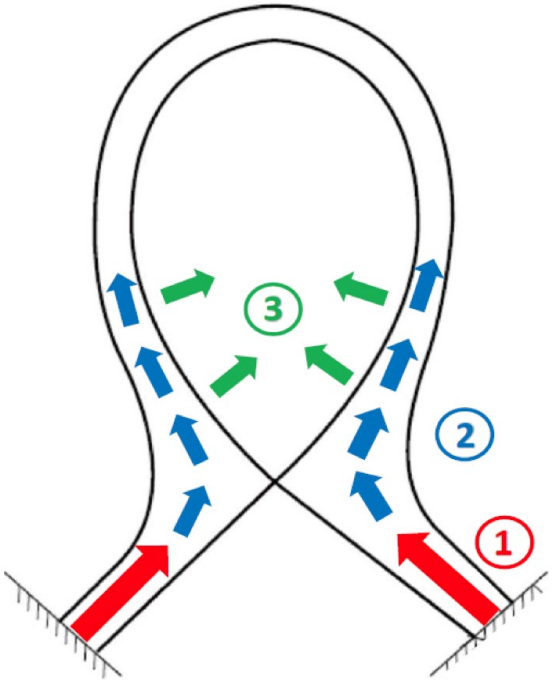

*e.g., in JET-ILW see Fedorczak et al., JNM, 2015

Basic metrics* in helping to understand impurity chain links:

① **Source Strength:**

Γ_w^{tile} [$m^{-2}s^{-1}$]

② **Divertor Retention Efficiency; source contamination of LCFS:**

$\eta_W^{LCFS} \equiv n_W(\rho=1)/\ \Gamma_W^{tile}$ [sm^{-1}]

③ **Core Contamination Efficiency; source contamination of core:**

$\eta_W^{Core} \equiv n_W(\rho=0)/\Gamma_W^{tile}$ [sm^{-1}]

For W, Ion Temperature Gradient (FiG) believed to play key part in causing SOL divertor leakage

SOL Impurity Parallel Force Balance

$$F_z = -\frac{1}{n_z}\frac{dp_z}{ds} + m_z\frac{(v_i - v_z)}{\tau_s} + ZeE + \alpha_e\frac{d(kT_e)}{ds} + \beta_i\frac{d(kT_i)}{ds} + \sim$$

FF FE FeG FiG

- FiG is especially strong for W: $\beta_i \sim 2.6Z^2$, for T > 30 eV, $\overline{Z}_W > 10$ (C.E.)
- Also β_i is not dependent on collisionality.
- FF is dependent on collisionality: $\tau_s \propto T_i^2/n$.

300 *Plasma Impurities*

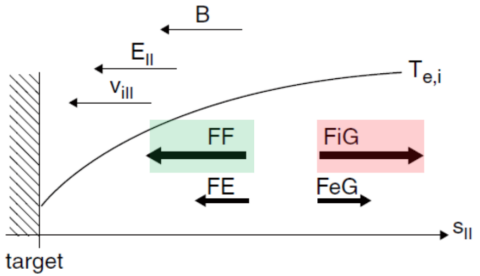

Figure 6.11. The principal parallel forces acting on impurity ions in the SOL. The friction, FF, and electrostatic, FE, forces are usually toward the target while the electron- and ion-temperature gradient forces, FeG, FiG, are usually away. Typically |FF| > |FE|, |FiG| > |FeG|.

Taken from: Stangeby, The Plasma Boundary of Magnetic Fusion Devices (2001)

More information at Unterberg, et. al., Nuclear Fusion (2019)

DIII-D Metal Rings Campaign used W sources localized to 2 poloidal locations in Outer Lower Divertor Region

- Isotopically distinct W sources allow impurities from each ring to act as unique ‘tracer’ particles.
- Using the same element eliminates differences in sputtering, conductivity, etc.
- Use of isotopes necessitates mass spectroscopy because RBS only discriminates elements.

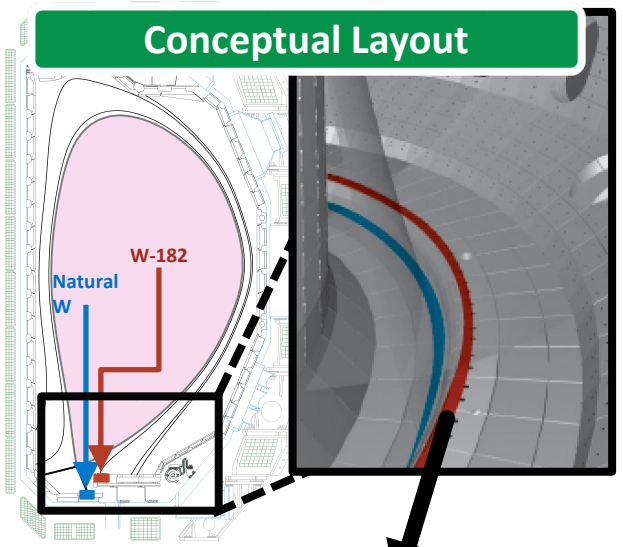

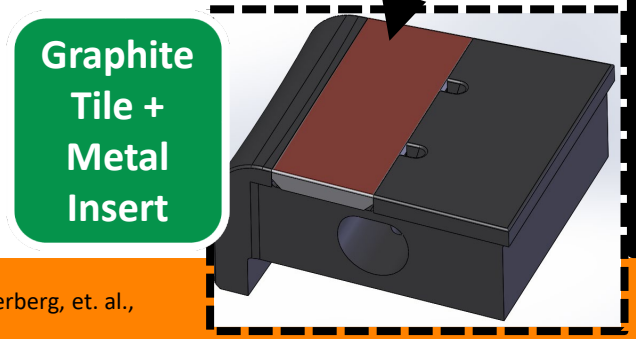

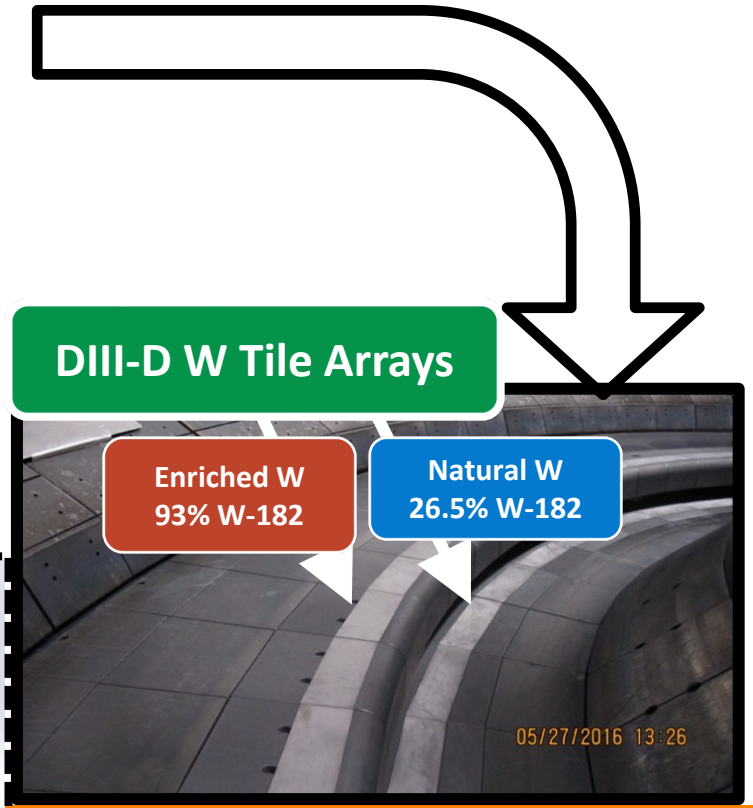

Holtrop, et. al., Fus. Sci. Tech. (2017); Unterberg, et. al., PFMC 2017-Dusseldorf

Collector probes inserted into the Far SOL region of DIII-D to study link in impurity transit chain

- Impurity transport in SOL best visualized using 1-D model.
- Impurity flux in Far SOL is contributed from core leakage and the near-SOL.

Probes have collecting faces on opposite sides normal to field lines:
- **Outer Target Face (OTF)**
- **Inner Target Face (ITF)**

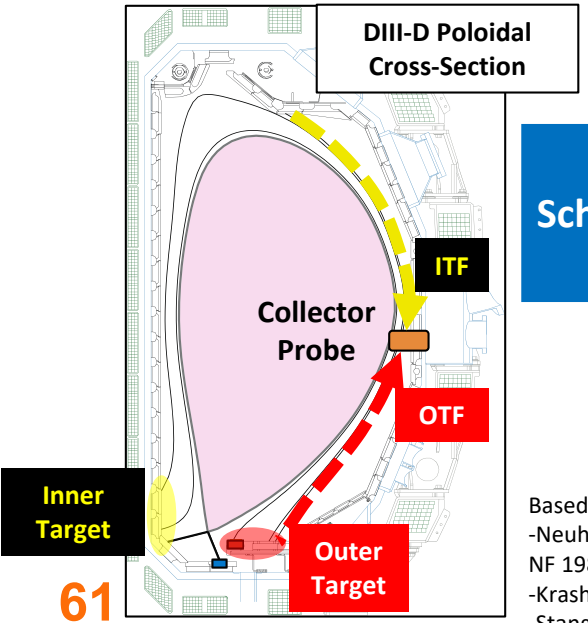

Simplified 1-D Schematic of DIV/SOL Fluxes

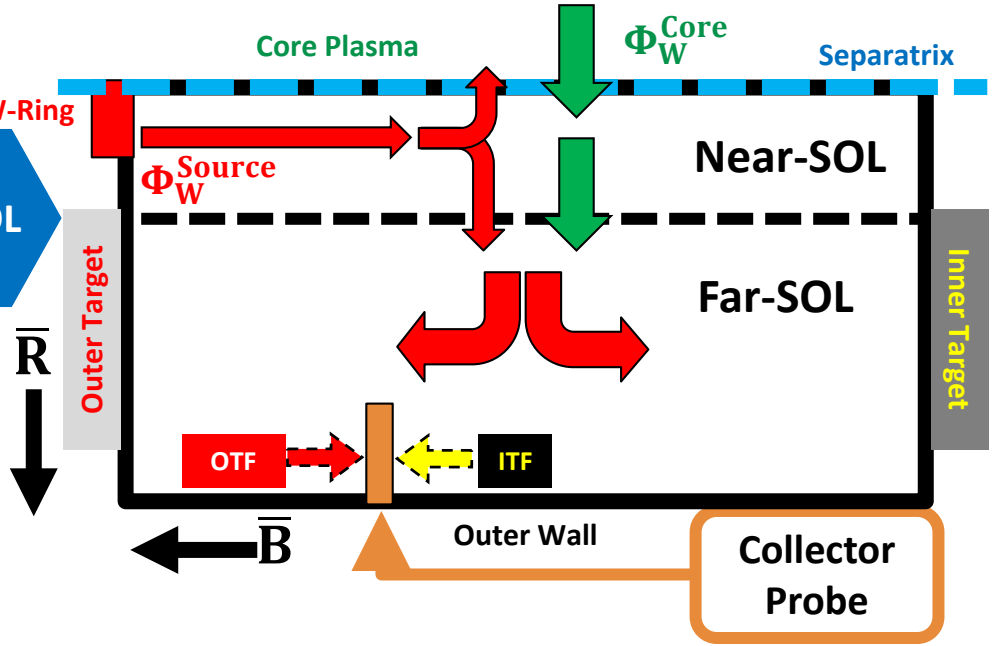

Based on:
-Neuhauser, Lackner, et al, NF 1984
-Krashenninikov et al, NF 1991
-Stangeby & Elder, NF 1995

DIII-D collector probe used unique triplet design allowing different sampling lengths to be employed

- Probe holder installed on DIII-D Mid-plane Reciprocating Probe drive (operated by UCSD*)
- 3 graphite probes with different diameters sample W-outfluxes over different parallel (thus also poloidal) spans.
- Probe axis normal to B field lines; collection faces on opposite sides.

• Allows comparison of deposition profiles on opposing inner target facing (ITF) and outer target facing (OTF) sides of probes.

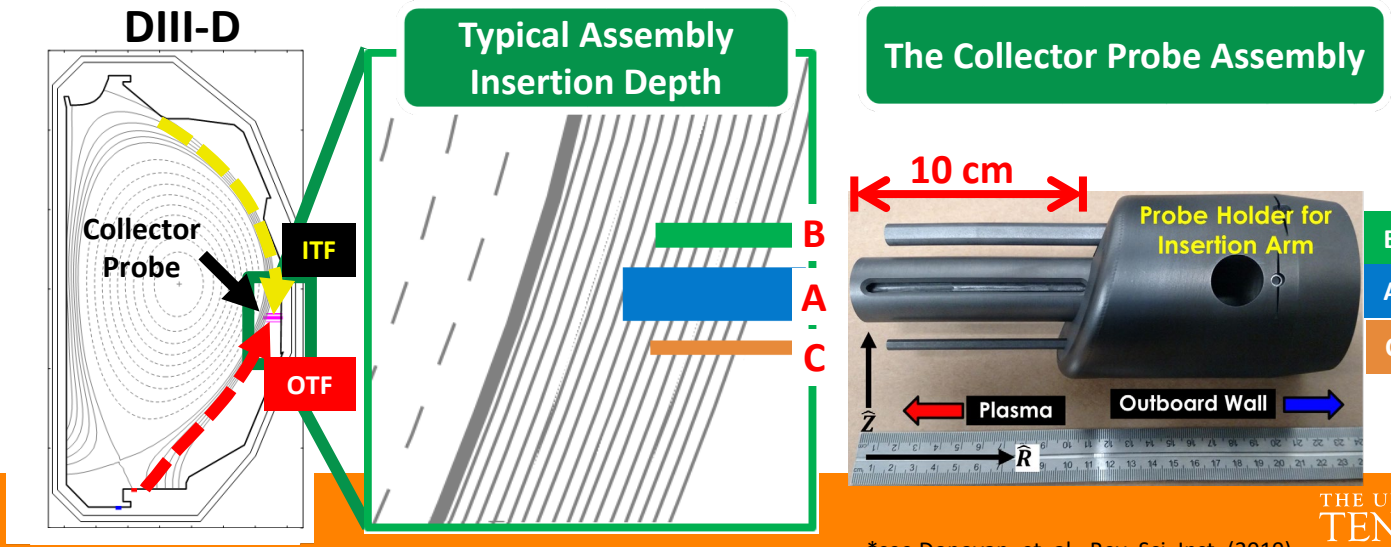

*see Donovan, et. al., Rev. Sci. Inst. (2019)

Collector probes measure impurity outfluxes in Far SOL, providing information pertinent to core leakage

- Collector probes intercept flux tubes in the far SOL and deplete particles over a finite length upstream and downstream (L_{samp}).
- Probe diameter (*d*) has strong influence on the sampling length.

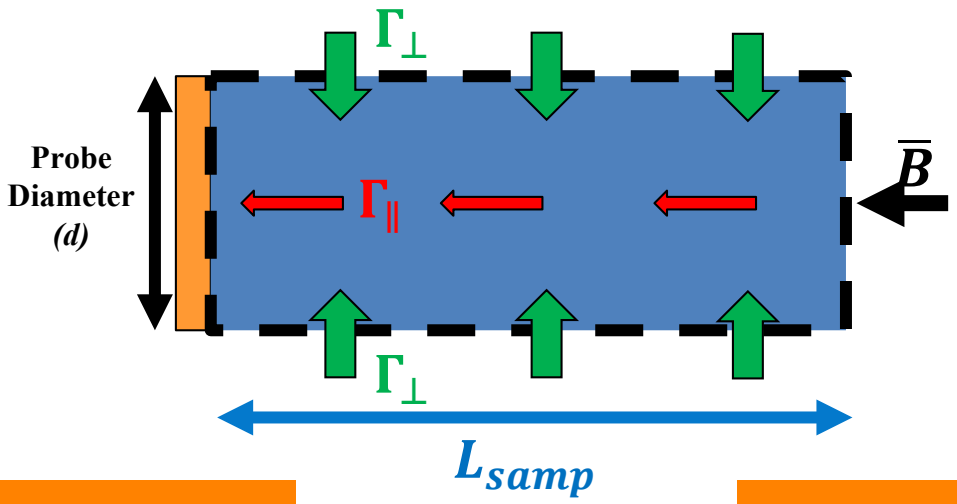

$$\Gamma_\perp = -D_\perp \frac{dn}{dr} \approx D_\perp \frac{n}{d}$$

$$\Gamma_\parallel = 0.5 n c_s$$

$$c_s = \left[\frac{k(T_e + T_i)}{m_i}\right]^{1/2}$$

Particle Balance

$$\Gamma_\parallel \times d = \Gamma_\perp \times 2L_{samp}$$

$$\frac{1}{2} n c_s d = D_\perp \frac{n}{d} 2L_{samp}$$

$$L_{samp} = \frac{c_s d^2}{4D_\perp}$$

- T_e is measured using Thomson scattering and plunging Langmuir probes.

Thickest probe samples regions of the SOL beyond the reach of the thinner probes

- Type A probe samples over a 4 m parallel span upstream and downstream.
- Types B, C probes sample over <1m parallel distance from the probe.

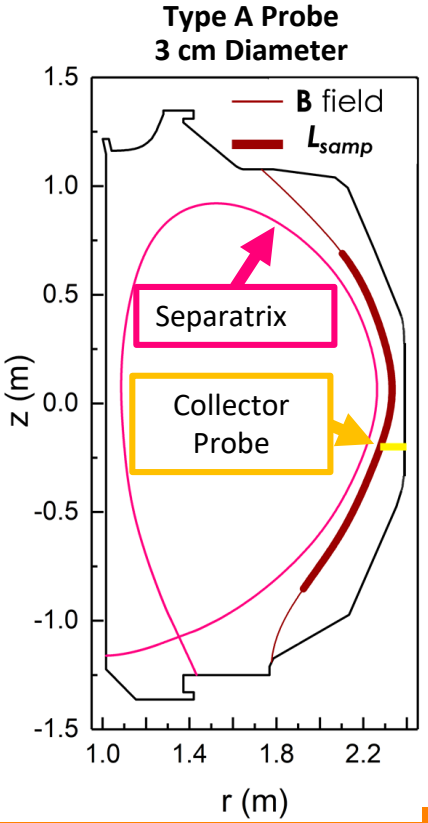

3-D Rendering of B Field Line and Sampling Length for Type A Probe

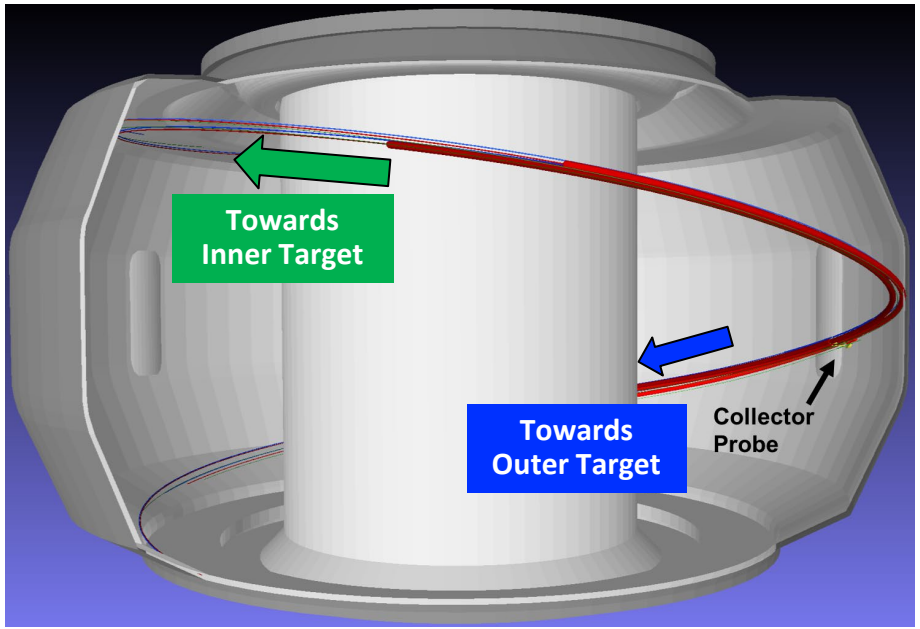

Higher W deposition on ITF side of 3 cm diameter probe appears to be first evidence for long theorized* impurity potential well in the SOL

Impurity transport in the edge plasma is dominated by a parallel force balance between:

Friction forces on impurity ions due to plasma flow **toward targets**

$\nabla_{\parallel} T_i$ forces on impurity ions **away from targets**

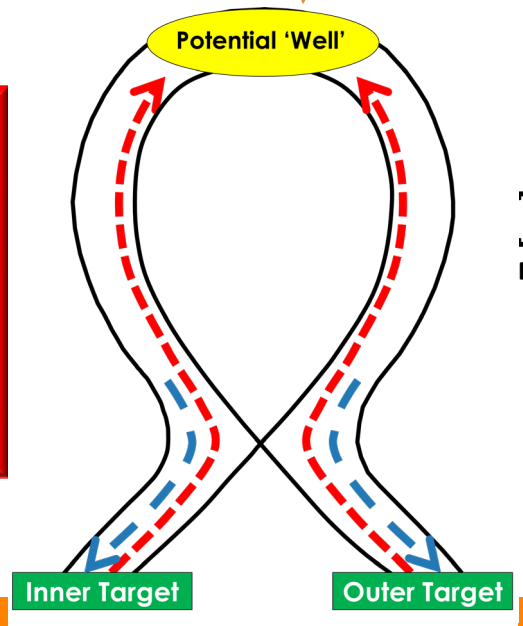

W impurity concentration due to 'well'

OEDGE/DIVIMP Computation Grid**

Type A Probe Sampling Length

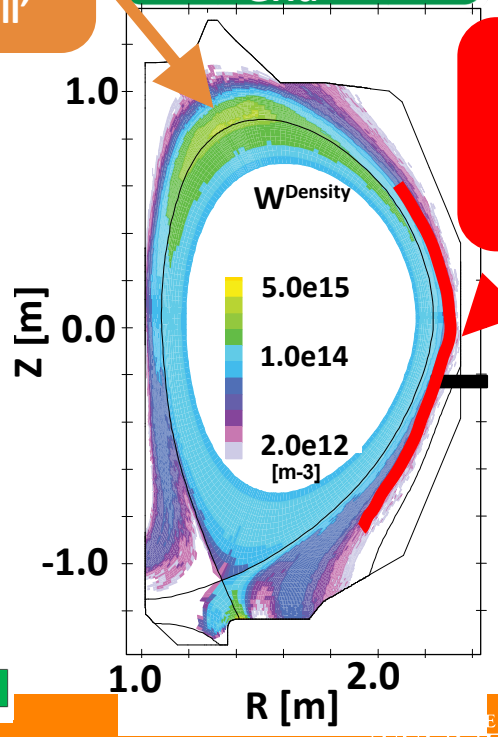

*see Stangeby, Elder, Nuclear Fusion (1995); Neuhauser, et. al., Nuclear Fusion (1984)
**Elder, et. al., J. Nuc. Mat. Energy (2019)

New focus on expanded use of DIVIMP-OEDGE-WallDYN (DOW) interpretive modeling suite at UTK-ORNL

- **DIVIMP: 2D Monte Carlo impurity transport**
  - Parallel forces
  - Collisions
  - ∥/⊥ Diffusion
  - Ioniz/Recomb
  - ExB drifts *NEW*

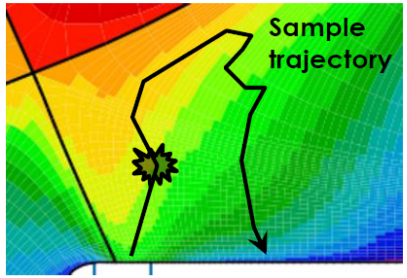

Stangeby NF 1995

Stangeby NME 2017

- **WallDYN: DIVIMP impurity transport with mixed-material surface evolution**

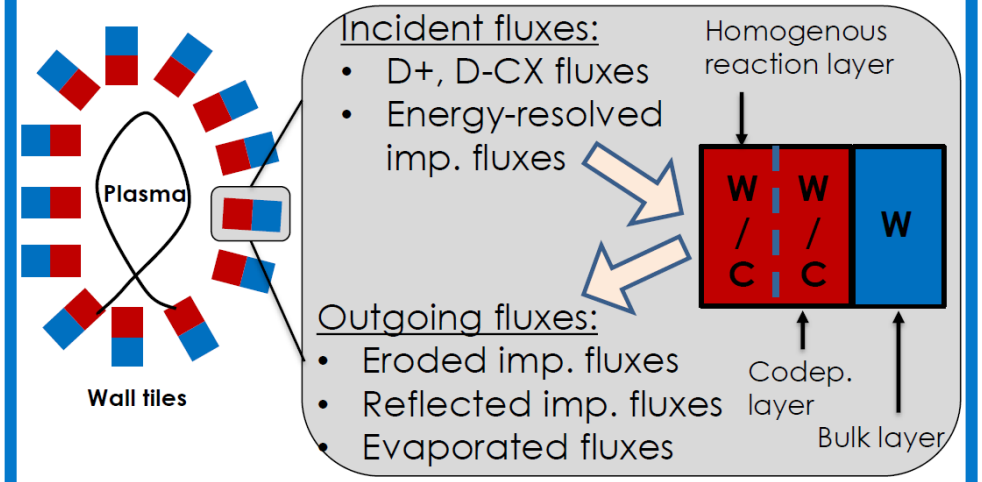

Flux balance gives impurity fluxes to wall and surface areal densities at each wall segment as function of time

Schmid JNM 2011

Schmid NF 2015

Nichols NME 2019

*Slide Credit to J. Nichols (UTK)

OEDGE plasma reconstruction serves as background for DIVIMP-WallDYN impurity model

Onion-skin fluid model matched to n_e and T_e from LPs and Thomson Scattering

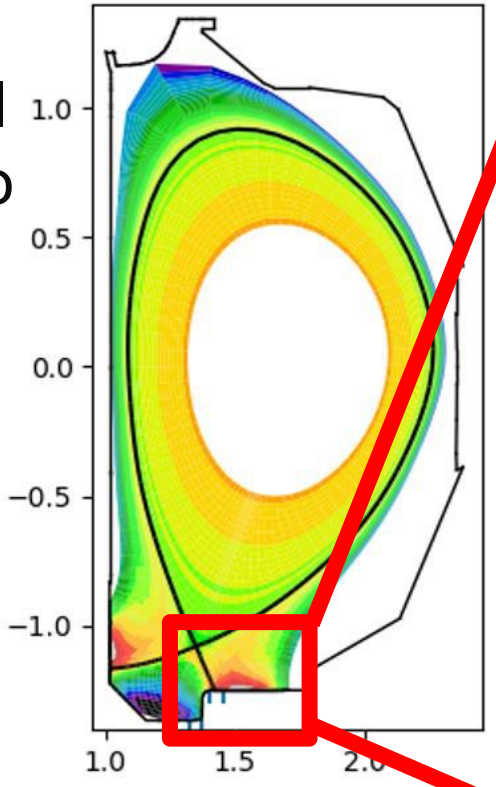

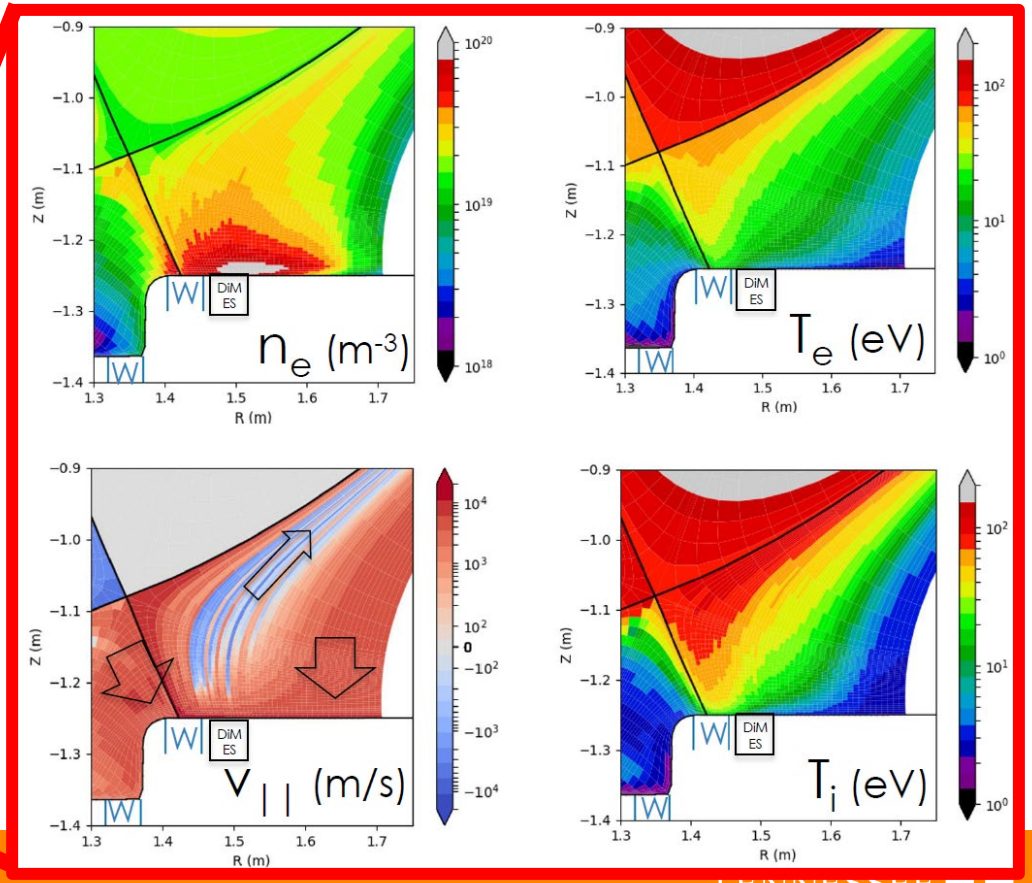

*Slide Credit to J. Nichols (UTK)

New features being added to DIVIMP-OEDGE to better account for drift effects in the edge plasma

Dr. Jacob Nichols (UTK) is leading new developments and uses of the DOW code suite on DIII-D and WEST

- DOE Postdoctoral Fellow
- PhD, Princeton University

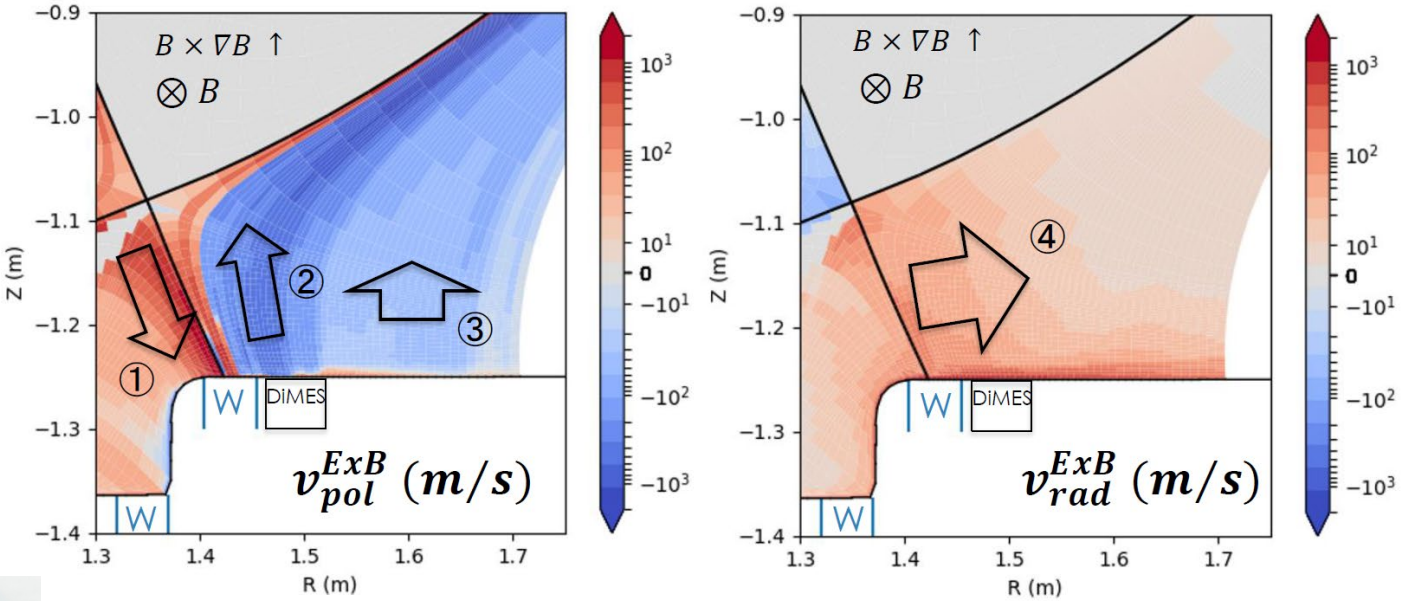

① Strong target-directed poloidal drifts very near separatrix
② Strong upstream-directed poloidal drifts in near SOL
③ Weak upstream-directed poloidal drifts in far SOL
④ Weak outward-directed radial drifts throughout

*Slide Credit to J. Nichols (UTK)

Acknowledgements

The authors would like to acknowledge the contributions of the UT Institute for Nuclear Security for providing access to essential equipment and personnel. This work was supported by the US Department of Energy under DE-SC0016318 (UTK), DE-SC0019256 (ECA), DE-AC05-00OR22725 (ORNL), DE-FG02-07ER54917 (UCSD), DE-FC02-04ER54698 (General Atomics), DE-NA0003525 (SNL).